Journal of Computational and Applied Mathematics 409 (2022) 114158

Contents lists available at ScienceDirect

Journal of Computational and Applied Mathematics

journal homepage: www.elsevier.com/locate/cam

Stability analysis and error estimates of fully-discrete local discontinuous Galerkin methods for simulating wormhole propagation with Darcy–Forchheimer model ☆

Lulu Tian [a], Hui Guo [a], Rui Jia [a], Yang Yang [b,*]

[a] College of Science, China University of Petroleum, Qingdao 266580, China
[b] Department of Mathematical Sciences, Michigan Technological University, Houghton, MI 49931, USA

ARTICLE INFO

Article history:
Received 25 August 2021
Received in revised form 26 December 2021

MSC:
65M15
65M60

Keywords:
Local discontinuous Galerkin method
Stability
Error estimates
Compressible wormhole propagation
Darcy–Forchheimer model

ABSTRACT

In this paper, we apply local discontinuous Galerkin (LDG) methods to compressible wormhole propagation with Darcy–Forchheimer model. We consider two time integrations up to second-order accuracy and prove the stability of the fully-discrete schemes. There are several difficulties. Firstly, different from most previous works discussing stability of wormhole propagations, we use LDG methods and have to deal with the inter-element discontinuities, leading to more complicated theoretical analysis. Secondly, in most previous stability analysis of LDG methods, a key step is to construct the relationship between the derivatives of the primitive variable and the auxiliary variables. This idea works for linear problems. However, our system is highly nonlinear and all the variables are coupled together. As an alternative, we will introduce a new auxiliary variable containing both the convection and diffusion terms. Thirdly, we have to control the change of the porosity during time evolution to obtain physically relevant numerical approximations and uniform upper bounds. Fourthly, to handle the time level mismatch of the spatial discretization due to the time integrations, we will construct a special second-order time method. Finally, to handle the complexity due to the Forchheimer term, we extrapolate some non-essential variables to linearize the coupled system, avoiding complicated iterations. To the best knowledge of the authors, this is the first scheme with time accuracy greater than one discussing stability for wormhole propagations. Moreover, we will prove the optimal error estimates of the schemes under mild time step restrictions. Numerical experiments are also given to verify the theoretical results.

© 2022 Elsevier B.V. All rights reserved.

1. Introduction

Acid treatment technique of carbonate reservoirs has been introduced and applied widely in the product enhancement of oil and gas reservoirs for the past few years. The main purpose of the process is to promote production rate by increasing permeability in the nearby damaged area. The acid is injected to dissolve the rocks near the wellbore, establishing flow channels that provide good connectivity between the reservoir and the well. Such channels are called wormholes.

☆ The first author was supported by the National Natural Science Foundation of China grant 11801569 and the second author was supported by the Major Scientific and Technological Projects of CNPC under Grant ZD2019-184-001. The last author was supported by NSF grant DMS-1818467.

* Corresponding author.
E-mail addresses: Tianll@upc.edu.cn (L. Tian), sdugh@163.com (H. Guo), UPCJiaRui@163.com (R. Jia), yyang7@mtu.edu (Y. Yang).

https://doi.org/10.1016/j.cam.2022.114158
0377-0427/© 2022 Elsevier B.V. All rights reserved.

There are many works discussing numerical simulation of wormhole propagations. The finite element method and the finite difference method were combined by Zhao et al. to analyze the chemical-dissolution front instability theoretically and numerically in [1]. Subsequently, a 3D simulation of carbonate acidization was investigated in [2]. Later, in [3], the authors applied parallel simulation. Moreover, the second-order block-centered finite difference method to simulate wormhole propagation has been developed in [4]. Recently, the characteristic splitting mixed finite element method was constructed in [5].

Most of the previous works for wormhole propagation are based on Darcy's framework. It is applicable for scenarios where porosity does not change significantly. However, when the porosity changes widely, it will result in high velocity of the fluid in the high-porosity region. In this case, the solution may deviate from reality. Therefore, the Darcy–Forchheimer model [6] was suggested to account for the case with nonuniform porosity and high velocity. There were several works discussing numerical solvers for the Darcy–Forchheimer model [7–13]. In addition, the mixed finite element method was applied to the Darcy–Forchheimer model and the stability was well studied [14]. However, this result was only limited to a semi-discrete framework. Moreover, a fully conservative block centered finite difference method was considered in [15]. However, only the first-order time scheme was investigated. In this paper, we will construct a second-order time integration and prove its stability and accuracy. Due to the significant differences in velocity, we need to consider methods with high resolutions. Therefore, we employ the discontinuous Galerkin (DG) method in this paper.

The DG method has gained greater popularity in recent decades due to its high order accuracy, local solvability and flexibility on hp-adaptivity. The method was first introduced by Reed and Hill [16] in the framework of neutron linear transport. Later, motivated by the work of Bassi and Rebay [17], Cockburn and Shu developed the local discontinuous Galerkin (LDG) method to solve the convection–diffusion equations in [18]. The main idea of the LDG method is to rewrite the equations with high-order derivatives into an equivalent first-order system. Then it is possible to apply the DG method to each equation in the new system. Therefore, the LDG method shares all the advantages of the DG method. Recently, the LDG method has been applied to conventional Darcy [19] and Darcy–Forchheimer model [20]. However, they were also limited to semi-discrete frameworks and the stability was missing.

In [21–23], the authors incorporated the IMEX time integrations with LDG methods for linear convection–diffusion problems, yielding good stability and accuracy. The basic idea was to introduce an auxiliary variable for the derivative of the primitive variable and establish the relationship between them. Then it is possible to use the diffusion term to control the convection term. For nonlinear problems, the stability was only demonstrated numerically, and the theoretical analysis was totally missing [24]. Later, the IMEX scheme was further applied to incompressible miscible displacements in [25]. However, only error estimates were discussed and no stability analysis was performed. Recently, we have applied LDG methods to Darcy's model with a first-order time integration and obtained the stability [26]. For second-order time integrations, the error estimates were obtained with the help of the *a priori* error estimates and the stability was also missing. In this paper, we will construct two special time integrations up to second-order accuracy for a more complicated Darcy–Forchheimer model and obtain the stability and error estimates for both schemes with mild time step restrictions. To the best knowledge of the authors, this is the first paper discussing stability of a second-order time integration for wormhole propagation.

There are five main difficulties in the theoretical analysis of our proposed methods. Firstly, different from [14,15], we use LDG methods for spatial discretization. Therefore, the theoretical analysis would be more difficult to perform since we need to deal with the inter-element discontinuities. Secondly, since our model is nonlinear and the variables are strongly coupled, it is difficult to follow [21–23] to obtain stability. In this paper, we will introduce a new auxiliary variable that contains both convection term and diffusion term. Moreover, following [14], we define an auxiliary function of velocity and establish its properties. With these properties, we could handle the analysis complication from the new auxiliary variable. Thirdly, we need to control the change of porosity to obtain physically relevant numerical porosity. Since the time evolution of the porosity does not interact with the spatial derivatives, we do not project it into the finite element space, but to apply a special way for the time integration. Moreover, we define a cut-off operator for the solute concentration which will not cause loss of accuracy, to control the growth rate of the porosity. Based on this operator, we get the uniform boundedness and monotonicity of the porosity for both first- and second-order time integrations. Especially, the uniform upper bounds are strictly less than one. Fourthly, we need to deal with the time level mismatch of the spatial discretizations. For first-order time integrations, the mismatch only appears in the porosity and this can be handled perfectly thanks to the monotonicity of porosity [26]. However, for most second-order time integrations, such as Crank–Nicolson method, the time level mismatch will appear in both porosity and velocity following the traditional LDG spatial discretization. Due to the lack of control of velocity, the spatial discretizations cannot be canceled or combined following the stability analysis in the semi-discrete frameworks. The main reason is that the time integration of the primitive variable is symmetric about time level $t^{n+1/2}$, while the auxiliary variable was given at both time levels t^n and t^{n+1}. To fix this, we will construct a special one-step time integration which is symmetric about time level $t^{n+1/2}$ for both the primitive and auxiliary variables to handle the mismatch. With the new time integration, the spatial discretizations of the primitive and auxiliary variables can be perfectly canceled. Finally, we have to deal with the Forchheimer term in the second-order time integration. Since the problem is highly nonlinear, the scheme would be extremely difficult to implement and some iterations should be performed. However, the convergence of those iterations can hardly be guaranteed theoretically and the iterations may be quite time consuming. To prompt efficient implementation, we modify the one-step time integration discussed above and use the values at time levels t^n, t^{n-1} to extrapolate some non-essential variables at time level t^{n+1} or $t^{n+1/2}$, which helps linearize the scheme and saves cost, keeping the stability and error estimates. Thanks to the stability, we can obtain the optimal error estimate in $L^\infty\left(L^2\right)$ for both schemes for concentration, velocity, pressure and porosity without any *a priori* error estimates.

The rest of the paper is organized as follows. In Section 2, we demonstrate the governing equations of the compressible wormhole propagation with Darcy–Forchheimer model. We present some preliminaries in Section 3, including the basic notations, norms and projections to be used throughout the paper. Two time integrations will be presented in Section 4, and the stability will also be proved. We give the error estimates in Section 5. Numerical results are provided to demonstrate the accuracy and capability of the method in Section 6. We will end in Section 7 with some concluding remarks.

2. Compressible wormhole propagation with Darcy-Forchheimer model

The governing equations of the compressible wormhole propagation over the computational domain $\Omega = [0, 1]\times[0, 1]$ are given by [14,15]:

$$\gamma\frac{\partial p}{\partial t}+\frac{\partial\phi}{\partial t}+\nabla\cdot\mathbf{u}=f, \tag{2.1}$$

$$\frac{\rho}{\phi}\frac{\partial\mathbf{u}}{\partial t}+\frac{\mu}{\kappa(\phi)}\mathbf{u}+\frac{\rho F(\phi)}{\sqrt{\kappa(\phi)}}|\mathbf{u}|\,\mathbf{u}=-\triangledown p+\rho\mathbf{g}, \tag{2.2}$$

$$\frac{\partial(\phi c_f)}{\partial t}+\nabla\cdot(\mathbf{u}c_f)-\nabla\cdot(\phi\mathbf{D}(\mathbf{u})\nabla c_f)=f_pc_f+f_Ic_I+k_ca_v(c_s-c_f), \tag{2.3}$$

$$\frac{\partial\phi}{\partial t}=\frac{\alpha k_ca_v(c_f-c_s)}{\rho_s}, \tag{2.4}$$

where p is the pressure in the fluid mixture, $\mathbf{u}$ is the Darcy velocity, ϕ is the porosity of the rock, c_f is the cup-mixing concentration of the acid in the fluid phase and κ is the permeability. ρ and $\mathbf{g}$ are the mass density and gravity vector, respectively. $F(\phi)=\frac{1.75}{\sqrt{150\phi^3}}$ is the Forchheimer number. Moreover, γ is a pseudo-compressibility parameter that contributes to minor change of the density of the fluid phase in the dissolution process. f gives the external volumetric flow rate consists of the injection rate f_I and production rate f_p. μ is the viscosity. c_I is the injected concentration. $\mathbf{D}$, the effective dispersion tensor, is defined as

$$\mathbf{D}(\mathbf{u})=d_m\mathbf{I}+|\mathbf{u}|\left\{\alpha_l\mathbf{E}(\mathbf{u})+\alpha_t\left(\mathbf{I}-\mathbf{E}(\mathbf{u})\right)\right\}, \tag{2.5}$$

$$(\mathbf{E}(\mathbf{u}))_{ij}=\frac{u_iu_j}{|\mathbf{u}|^2},\quad 1\le i,j\le 2,$$

where $d_m > 0$ is the molecular diffusivity. The longitudinal and the transverse dispersivities α_l and α_t are positively defined. It is easy to see that $\mathbf{D(u)}$ is an invertible positive definite matrix. k_c is the coefficient of local mass-transfer and c_s is the acid concentration at the fluid–solid interface. There is a relationship between c_s and c_f given as

$$c_s=\frac{c_f}{1+k_s/k_c}, \tag{2.6}$$

where k_s is the rate of surface reaction. The porosity ϕ and the permeability κ have the following relationship

$$\frac{\kappa}{\kappa_0}=\frac{\phi}{\phi_0}\left(\frac{\phi(1-\phi_0)}{\phi_0(1-\phi)}\right)^2, \tag{2.7}$$

which is established by the Carman–Kozeny correlation [27], where κ_0 and ϕ_0 are the initial permeability and porosity, respectively. Clearly, κ is a function of ϕ and

$$\frac{1}{\kappa(\phi)}=\kappa^{-1}(\phi)=\frac{\phi_0}{\phi\kappa_0}\left(\frac{\phi_0(1-\phi)}{\phi(1-\phi_0)}\right)^2. \tag{2.8}$$

In (2.4), ρ_s is the density of the solid phase, α is the dissolving power of the acid, a_v is the interfacial area available for reaction per unit volume of the medium and it can be calculated as

$$\frac{a_v}{a_0}=\frac{\phi}{\phi_0}\sqrt{\frac{\kappa_0\phi}{\kappa\phi_0}}=\frac{1-\phi}{1-\phi_0}, \tag{2.9}$$

with a_0 being the area of initial interfacial. Moreover, the initial solutions are given as

$$c_f(x,y,0)=c_0(x,y),\quad \phi(x,y,0)=\phi_0(x,y),\quad p(x,y,0)=p_0(x,y),\quad \mathbf{u}(x,y,0)=\mathbf{u}_0(x,y).$$

In this paper, we consider periodic boundary conditions for simplicity. The problem with homogeneous Neumann boundary conditions can be analyzed with some minor changes, so we omit it.

Finally, we would like to make the following hypotheses (H) for the problem.

1. $0 < \phi_* \leq \phi(x, y, t) \leq \phi^* < 1$.
2. $\gamma, \alpha, \rho, \rho_s, \mu, k_c$, and k_s are all given positive constants, and $0 < a_{0*} \leq a_0 \leq a_0^*$.
3. c_f, c_{f_t}, $\mathbf{u}$, $\mathbf{u}_t$ and $\mathbf{s}$ are uniformly bounded in $R^2 \times [0, T]$.

The following lemma follows from direct computation, hence we demonstrate the result only and skip the proof.

Lemma 2.1. *$\kappa^{-1}(\phi)$, $a_v(\phi)$ and $F(\phi)$ are Lipschitz continuous, i.e. there exists $C > 0$ such that*

$$|\kappa^{-1}(\phi_1) - \kappa^{-1}(\phi_2)| \leq C|\phi_1 - \phi_2|, \quad |a_v(\phi_1) - a_v(\phi_2)| \leq C|\phi_1 - \phi_2|, \quad |F(\phi_1) - F(\phi_2)| \leq C|\phi_1 - \phi_2|.$$

3. Preliminaries

In this section, we will demonstrate some basic notations and projections to be used in the rest of the paper.

3.1. Basic notations

Let $0 = x_{\frac{1}{2}} < x_{\frac{3}{2}} < \cdots < x_{N_x+\frac{1}{2}} = 1$ and $0 = y_{\frac{1}{2}} < y_{\frac{3}{2}} < \cdots < y_{N_y+\frac{1}{2}} = 1$ be the grid points in x and y directions, respectively. We consider a rectangular partition $\Omega_h = \left\{K_{ij}\right\}_{i=1,2,\ldots,N_x}^{j=1,2,\ldots,N_y}$ of Ω and define

$$K_{ij} = I_i \times J_j, \quad i = 1, \ldots, N_x,\ j = 1, \ldots, N_y,$$

where $I_i = [x_{i-\frac{1}{2}}, x_{i+\frac{1}{2}}]$ and $J_j = [y_{j-\frac{1}{2}}, y_{j+\frac{1}{2}}]$. Define $h_i^x = x_{i+\frac{1}{2}} - x_{i-\frac{1}{2}}$, $h_j^y = y_{j+\frac{1}{2}} - y_{j-\frac{1}{2}}$ as the mesh sizes in x and y directions, respectively, and denote $h = \max_{i,j}(h_i^x, h_j^y)$. In this paper, the partition is assumed to be quasi-uniform, i.e. $\min_{i,j}\{h_i^x, h_j^y\} \leq h \leq C \min_{i,j}\{h_i^x, h_j^y\}$ for some positive constant C.

We choose the finite element space as

$$W_h^k = \{z : z|_K \in Q^k(K), \forall K \in \Omega_h\},$$

where $Q^k(K)$ denotes the space of tensor product polynomials of degree at most k in K. Denote Γ_h as the set of all element interfaces and define $\Gamma_0 = \Gamma_h \backslash \partial\Omega$. $\boldsymbol{\beta} = (1, 1)^T$ is a predetermined vector. Let $\mathcal{E} \in \Gamma_0$ be an interior edge, and it is shared by two elements K_ℓ and K_r, where $\boldsymbol{\beta} \cdot \mathbf{n}_\ell > 0$, and $\boldsymbol{\beta} \cdot \mathbf{n}_r < 0$, with $\mathbf{n}_\ell$ and $\mathbf{n}_r$ being the outward normals of K_ℓ and K_r. For any $s \in W_h^k$, s^- and s^+ represent the values of s taken from K_ℓ and K_r, respectively. Furthermore, the jump is given as $[s] = s^+ - s^-$. Moreover, for $\mathbf{z} \in \mathbf{W}_h^k = W_h^k \times W_h^k$, $\mathbf{z}^+$, $\mathbf{z}^-$ and $[\mathbf{z}]$ are defined analogously. More details can be found in [19].

We use the traditional notation $L^p(K)$, $1 \leq p \leq \infty$, for the L^p space over K, equipped with norm $\|\cdot\|_{p,K}$. For simplicity, if $K = \Omega$ or $p = 2$, we will omit the corresponding subscript. Moreover, we define several inner products

$$(u, v)_K = \int_K uv\,dxdy, \quad (\mathbf{u}, \mathbf{v})_K = \int_K \mathbf{u} \cdot \mathbf{v}\,dxdy, \quad \langle u, v\rangle_{\partial K} = \int_{\partial K} uv\,ds.$$

Let Γ_K be the edges of K, and we define $\|\cdot\|_{\Gamma_K}^2 = \langle \cdot, \cdot \rangle_{\partial K}$ and $\|\cdot\|_{\Gamma_h}^2 = \sum_K \|\cdot\|_{\Gamma_K}^2$. Throughout this paper, we use C as a generic constant independent of time step and mesh size, and it may have different values at different occurrences. Moreover, ε is a sufficiently small positive constant.

3.2. Projections

We will define several special projections and demonstrate their properties. Before doing so, let us start with the classical inverse property [28].

Lemma 3.1. *Suppose $u \in W_h^k$, then there exists a positive constant C independent of u such that*

$$h\,\|u\|_{\infty,K} + h^{1/2}\,\|u\|_{\Gamma_K} \leq C\,\|u\|_K\,.$$

Now we define P^+ into W_h^k which is, for each cell K

$$(P^+u - u, v)_K = 0,\ \ \forall v \in Q^{k-1}(K), \qquad \int_{J_j}(P^+u - u)(x_{i-\frac{1}{2}}, y)v(y)dy = 0,\ \ \forall v \in P^{k-1}(J_j),$$

$$\int_{I_i}(P^+u - u)(x, y_{j-\frac{1}{2}})v(x)dx = 0,\ \ \forall v \in P^{k-1}(I_i), \qquad (P^+u - u)(x_{i-\frac{1}{2}}, y_{j-\frac{1}{2}}) = 0,$$

where $P^k(I)$ denotes the kth degree polynomials over the interval I. Moreover, we define Π_x^- and Π_y^- into W_h^k which are, for each cell K,

$$(\Pi_x^- u - u, v_x)_K = 0, \ \forall v \in Q^k(K), \qquad \int_{J_j} (\Pi_x^- u - u)(x_{i+\frac{1}{2}}, y)v(y)dy = 0, \ \forall v \in P^k(J_j),$$
$$(\Pi_y^- u - u, v_y)_K = 0, \ \forall v \in Q^k(K), \qquad \int_{I_i} (\Pi_y^- u - u)(x, y_{j+\frac{1}{2}})v(x)dx = 0, \ \forall v \in P^k(I_i),$$

as well as a vector-valued projection $\mathbf{\Pi}^- = \Pi_x^- \otimes \Pi_y^-$. The following lemma gives the error of the projections [28].

Lemma 3.2. *Assume $w \in H^{k+1}(\Omega)$, $k \geq 1$, then for any projection P_h, which is either P^+, Π_x^- or Π_y^-, we have*

$$\|w - P_h w\| + h^{1/2} \|w - P_h w\|_{\Gamma_h} \leq Ch^{k+1}.$$

Moreover, the following superconvergence property works for the projection P^+ on Cartesian meshes [29].

Lemma 3.3. *Let $w \in H^{k+2}(\Omega)$, then for any K and $\boldsymbol{\rho} \in \mathbf{W}_h^k$ we have*

$$\left|\left(w - P^+ w, \nabla \cdot \boldsymbol{\rho}\right)_K - \left\langle w - P^+ w, \boldsymbol{\rho} \cdot \boldsymbol{n}_K\right\rangle_{\partial K}\right| \leq Ch^{k+1} \|w\|_{k+2} \|\boldsymbol{\rho}\|_K ,$$

where $\boldsymbol{n}_K$ is the outward normal of K, and $C > 0$ is independent of K.

Before we finish this section, we would like to demonstrate the following lemma whose proof was given in [30].

Lemma 3.4. *Define $u \in C^{k+1}(\Omega)$ and $\Pi u \in W_h^k$. Suppose $\|u - \Pi u\| \leq Ch^\kappa$ for $\kappa \leq k + 1$. Then*

$$h \|u - \Pi u\|_\infty + h^{1/2} \|u - \Pi u\|_{\Gamma_h} \leq Ch^\kappa.$$

4. LDG schemes

In this section, we will present the LDG schemes. We will start from the semi-discrete scheme.

4.1. Semi-discrete LDG scheme

Applying (2.6)–(2.9), we rewrite (2.1)–(2.4) into

$$\gamma \frac{\partial p}{\partial t} + \frac{\partial \phi}{\partial t} + \nabla \cdot \mathbf{u} = f, \tag{4.1}$$
$$\frac{\rho}{\phi} \frac{\partial \mathbf{u}}{\partial t} + \frac{\mu}{\kappa(\phi)} \mathbf{u} + \frac{\rho F(\phi)}{\sqrt{\kappa(\phi)}} |\mathbf{u}| \mathbf{u} = -\nabla p + \rho \mathbf{g}, \tag{4.2}$$
$$\frac{\partial(\phi c_f)}{\partial t} + \nabla \cdot \mathbf{s} + Aa_v(\phi)c_f = f_p c_f + f_I c_I, \tag{4.3}$$
$$\mathbf{s} = \mathbf{u}c_f - \phi \mathbf{D}(\mathbf{u}) \nabla c_f, \tag{4.4}$$
$$\frac{\partial \phi}{\partial t} = Ba_v(\phi) c_f, \tag{4.5}$$

where $A = \frac{k_c k_s}{k_c + k_s}$, $B = \frac{\alpha k_c k_s}{\rho_s(k_c + k_s)}$ and $a_v(\phi) = \frac{a_0(1-\phi)}{1-\phi_0}$. **s** is a new auxiliary variable which is crucial in the stability analysis. This idea was first developed in [14] in obtaining stability under a semi-discrete framework. Furthermore, we construct a function of velocity as

$$\mathbf{M}_e(\mathbf{u}) = (\mathbf{D}(\mathbf{u}))^{-1} \mathbf{u}, \tag{4.6}$$

and a cut-off operator $\mathcal{M}$ as

$$\mathcal{M}(\mathbf{u}) := \begin{cases} \mathbf{u}, & |\mathbf{u}| \leq S, \\ S\mathbf{u}/|\mathbf{u}|, & |\mathbf{u}| > S, \end{cases} \tag{4.7}$$

where the positive constant S is sufficiently large. The LDG scheme for (4.1)–(4.4) is as follows: Find p_h, $c_h \in W_h^k$ and $\mathbf{s}_h$, $\mathbf{u}_h \in \mathbf{W}_h^k$ such that for any $\zeta, v \in W_h^k$, $\boldsymbol{\theta}, \mathbf{w} \in \mathbf{W}_h^k$, we have

$$\left(\gamma \frac{\partial p_h}{\partial t}, \zeta\right)_K + \left(\frac{\partial \phi_h}{\partial t}, \zeta\right)_K = \mathcal{L}_K^d(\mathbf{u}_h, \zeta) + (f, \zeta)_K, \tag{4.8}$$
$$\left(\frac{\rho}{\phi_h} \frac{\partial \mathbf{u}_h}{\partial t}, \boldsymbol{\theta}\right)_K + \left(\frac{\mu}{\kappa(\phi_h)} \mathbf{u}_h, \boldsymbol{\theta}\right)_K + \left(\frac{\rho F(\phi_h)}{\sqrt{\kappa(\phi_h)}} |\mathbf{u}_h| \mathbf{u}_h, \boldsymbol{\theta}\right)_K = \mathcal{D}_K(p_h, \boldsymbol{\theta}) + (\rho \mathbf{g}, \boldsymbol{\theta})_K, \tag{4.9}$$

$$((\phi_h c_h)_t, v)_K = \mathcal{L}_K^d(\mathbf{s}_h, v) + (f_p c_h + f_I c_I, v)_K - (Aa_v(\phi_h)c_h, v)_K, \tag{4.10}$$

$$\left(\left(\phi_h \mathbf{D}(\mathbf{u}_h^M)\right)^{-1} \mathbf{s}_h, \mathbf{w}\right)_K = \left((\phi_h)^{-1} \mathbf{M}_e\left(\mathbf{u}_h\right) c_h, \mathbf{w}\right)_K + \mathcal{D}_K\left(c_h, \mathbf{w}\right), \tag{4.11}$$

where

$$\mathcal{L}_K^d(\mathbf{s}, v) = (\mathbf{s}, \nabla v)_K - \langle \widehat{\mathbf{s}} \cdot \boldsymbol{\nu}_K, v\rangle_{\partial K} \quad \text{and} \quad \mathcal{D}_K(c, \mathbf{w}) = (c, \nabla\cdot\mathbf{w})_K - \langle \widehat{c}, \mathbf{w}\cdot\boldsymbol{\nu}_K\rangle_{\partial K},$$

with $\mathbf{u}_h^M = \mathcal{M}(\mathbf{u}_h)$ and $\boldsymbol{\nu}_K$ being the unit outer normal of K. Since (4.5) is only an ordinary differential equation with respect to time, it is not necessary to perform spatial discretization. The time integration of the porosity is given as

$$\frac{\partial \phi_h}{\partial t} = Ba_v\left(\phi_h\right)\bar{c}_h, \tag{4.12}$$

where $\bar{c}_h$ =max(0,min $(c_h, 1)$). The hat terms in the LDG schemes are the numerical fluxes. In this paper, we choose

$$\widehat{\mathbf{s}_h} = \mathbf{s}_h^-, \quad \widehat{c_h} = c_h^+, \quad \widehat{\mathbf{u}_h} = \mathbf{u}_h^-, \quad \widehat{p_h} = p_h^+.$$

In addition, we define

$$(u, v) = \sum_{K\in\Omega_h}(u, v)_K, \qquad (\mathbf{u}, \mathbf{v}) = \sum_{K\in\Omega_h}(\mathbf{u}, \mathbf{v})_K, \qquad \mathcal{L}^d(\mathbf{s}, v) = \sum_{K\in\Omega_h}\mathcal{L}_K^d(\mathbf{s}, v), \qquad \mathcal{D}(c, \mathbf{w}) = \sum_{K\in\Omega_h}\mathcal{D}_K(c, \mathbf{w}).$$

With integration by parts, it is easy to check that for any v and $\mathbf{w}$, we have

$$\mathcal{L}^d(\mathbf{w}, v) + \mathcal{D}(v, \mathbf{w}) = 0. \tag{4.13}$$

4.2. Fully-discrete LDG schemes

We consider a uniform partition $\{t^n = n\tau\}_{n=0}^M$ of the time interval $[0, T]$, with time mesh size $\tau = T/M$. However, the assumption of uniform partition is not essential. Two time integrations coupled with LDG spatial discretization will be discussed.

4.2.1. First-order time integration

The first-order time integration, donated as Fully-LDG(k,1), will be constructed. For any $n \geq 0$, given the numerical solutions $c_h^n, p_h^n, \phi_h^n, \mathbf{u}_h^n, \mathbf{s}_h^n$ at time level n, we calculate ϕ_h^{n+1} by

$$\frac{\phi_h^{n+1} - \phi_h^n}{\tau} = Ba_v\left(\phi_h^{n+1}\right)\bar{c}_h^n. \tag{4.14}$$

Then $p_h^{n+1}, \mathbf{u}_h^{n+1}$ can be computed via

$$\left(\gamma\frac{p_h^{n+1} - p_h^n}{\tau}, \zeta\right) + \left(\frac{\phi_h^{n+1} - \phi_h^n}{\tau}, \zeta\right) = \mathcal{L}^d\left(\mathbf{u}_h^{n+1}, \zeta\right) + \left(f^n, \zeta\right), \tag{4.15}$$

$$\left(\frac{\rho}{\phi_h^{n+1}}\frac{\mathbf{u}_h^{n+1} - \mathbf{u}_h^n}{\tau}, \boldsymbol{\theta}\right) + \left(\frac{\mu}{\kappa(\phi_h^{n+1})}\mathbf{u}_h^{n+1}, \boldsymbol{\theta}\right) + \left(\frac{\rho F\left(\phi_h^{n+1}\right)}{\sqrt{\kappa\left(\phi_h^{n+1}\right)}}\left|\mathbf{u}_h^{n+1}\right|\mathbf{u}_h^{n+1}, \boldsymbol{\theta}\right) = \mathcal{D}(p_h^{n+1}, \boldsymbol{\theta}) + (\rho\mathbf{g}, \boldsymbol{\theta}), \tag{4.16}$$

for any $\zeta \in W_h^k, \boldsymbol{\theta} \in \mathbf{W}_h^k$. Finally, we can find $c_h^{n+1}, \mathbf{s}_h^{n+1}$ by

$$\left(\frac{\phi_h^{n+1}c_h^{n+1} - \phi_h^n c_h^n}{\tau}, v\right) = \mathcal{L}^d\left(\mathbf{s}_h^{n+1}, v\right) - \left(Aa_v\left(\phi_h^n\right)c_h^n, v\right) + \left(f_p^n c_h^n + f_I^n c_I^n, v\right), \tag{4.17}$$

$$\left(\left(\phi_h^{n+1}\mathbf{D}(\mathbf{u}_h^{n+1,M})\right)^{-1}\mathbf{s}_h^{n+1}, \mathbf{w}\right) = \left(\left(\phi_h^{n+1}\right)^{-1}\mathbf{M}_e\left(\mathbf{u}_h^{n+1}\right)c_h^{n+1}, \mathbf{w}\right) + \mathcal{D}\left(c_h^{n+1}, \mathbf{w}\right), \tag{4.18}$$

for any $v \in W_h^k, \mathbf{w} \in \mathbf{W}_h^k$. The initial approximations are

$$\phi_h(x, y, 0) = \phi(x, y, 0), \quad c_h(x, y, 0) = P^+c_0, \quad p_h(x, y, 0) = P^+p_0, \quad \mathbf{u}_h(x, y, 0) = \mathbf{\Pi}^-\mathbf{u_0}. \tag{4.19}$$

Remark 4.1. For simplicity of implementation, it is possible to replace $\frac{\rho F\left(\phi_h^{n+1}\right)}{\sqrt{\kappa\left(\phi_h^{n+1}\right)}}\left|\mathbf{u}_h^{n+1}\right|\mathbf{u}_h^{n+1}$ in (4.16) by $\frac{\rho F\left(\phi_h^{n+1}\right)}{\sqrt{\kappa\left(\phi_h^{n+1}\right)}}\left|\mathbf{u}_h^{n}\right|\mathbf{u}_h^{n+1}$. The alternative scheme is also stable and has the same accuracy.

4.2.2. Second-order time integration

We introduce a special second-order time integration, namely Fully-LDG(k,2). For any $n \geq 1$, given the numerical solutions at t^n, t^{n-1}, we first compute ϕ_h^{n+1} as

$$\frac{\phi_h^{n+1}-\phi_h^n}{\tau} = \frac{1}{2}Ba_v\left(\phi_h^{n+1}\right)\bar{c}_h^{n+1,*} + \frac{1}{2}Ba_v\left(\phi_h^n\right)\bar{c}_h^n, \tag{4.20}$$

where

$$c_h^{n+1,*} = \begin{cases} 2c_h^n - c_h^{n-1}, & n \geq 1, \\ c_h^0, & n = 0. \end{cases} \tag{4.21}$$

We extrapolate c_h^{n+1} to decouple the system. Otherwise, the numerical scheme may form a coupled system, and it is extremely difficult to implement. Then we obtain $p_h^{n+1}, \mathbf{u}_h^{n+1}$ via

$$\left(\gamma\frac{p_h^{n+1}-p_h^n}{\tau}, \zeta\right) + \left(\frac{\phi_h^{n+1}-\phi_h^n}{\tau}, \zeta\right) = \mathcal{L}^d\left(\frac{\mathbf{u}_h^{n+1}+\mathbf{u}_h^n}{2}, \zeta\right) + \left(f^{n+\frac{1}{2}}, \zeta\right), \tag{4.22}$$

$$\begin{aligned} &\left(\frac{\rho}{\phi_h^{n+\frac{1}{2}}}\frac{\mathbf{u}_h^{n+1}-\mathbf{u}_h^n}{\tau}, \boldsymbol{\theta}\right) + \left(\frac{\rho F\left(\phi_h^{n+\frac{1}{2}}\right)}{\sqrt{\kappa\left(\phi_h^{n+\frac{1}{2}}\right)}}\left|\frac{3\mathbf{u}_h^n-\mathbf{u}_h^{n-1}}{2}\right|\frac{\mathbf{u}_h^{n+1}+\mathbf{u}_h^n}{2}, \boldsymbol{\theta}\right) \\ &= -\left(\frac{\mu}{\kappa(\phi_h^{n+\frac{1}{2}})}\frac{\mathbf{u}_h^{n+1}+\mathbf{u}_h^n}{2}, \boldsymbol{\theta}\right) + \mathcal{D}\left(\frac{p_h^{n+1}+p_h^n}{2}, \boldsymbol{\theta}\right) + (\rho\mathbf{g}, \boldsymbol{\theta}), \end{aligned} \tag{4.23}$$

for any $\zeta \in W_h^k, \boldsymbol{\theta} \in \mathbf{W}_h^k$, where

$$\phi_h^{n+\frac{1}{2}} = \frac{\phi_h^{n+1}+\phi_h^n}{2}, \qquad \mathbf{u}_h^{n+\frac{1}{2}} = \frac{\mathbf{u}_h^{n+1}+\mathbf{u}_h^n}{2}, \qquad f^{n+\frac{1}{2}} = \frac{f^{n+1}+f^n}{2}.$$

For simplicity, we also use the above notation for f_p, f_I and c_I. In (4.23), extrapolation was applied in the absolute value to linearize the scheme. Finally, $c_h^{n+1}, \mathbf{s}_h^{n+1}$ are obtained through

$$\begin{aligned} \left(\frac{\phi_h^{n+1}c_h^{n+1}-\phi_h^n c_h^n}{\tau}, v\right) &= \mathcal{L}^d\left(\frac{\mathbf{s}_h^{n+1}+\mathbf{s}_h^n}{2}, v\right) - \left(Aa_v\left(\phi_h^{n+\frac{1}{2}}\right)\frac{c_h^{n+1}+c_h^n}{2}, v\right) \\ &\quad + \left(f_p^{n+\frac{1}{2}}\frac{c_h^{n+1}+c_h^n}{2} + f_I^{n+\frac{1}{2}}c_I^{n+\frac{1}{2}}, v\right), \end{aligned} \tag{4.24}$$

$$\left(\left(\phi_h^{n+\frac{1}{2}}\mathbf{D}\left(\mathbf{u}_h^{n+\frac{1}{2},M}\right)\right)^{-1}\frac{\mathbf{s}_h^{n+1}+\mathbf{s}_h^n}{2}, \mathbf{w}\right) = \left(\left(\phi_h^{n+\frac{1}{2}}\right)^{-1}\mathbf{M}_e\left(\mathbf{u}_h^{n+\frac{1}{2}}\right)\frac{c_h^{n+1}+c_h^n}{2}, \mathbf{w}\right) + \mathcal{D}\left(\frac{c_h^{n+1}+c_h^n}{2}, \mathbf{w}\right), \tag{4.25}$$

for all $v \in W_h^k, \mathbf{w} \in \mathbf{W}_h^k$.

Eq. (4.25) is quite different from all the previous LDG methods, since we did not discretize it at time level t^n. Actually, it is symmetric about time level $t^{n+\frac{1}{2}}$ and this is crucial in stability analysis as it can avoid time level mismatch of the spatial discretization. The initial solutions are given as follows. We take the solutions at t^0 from (4.19) and the solutions $\phi_h, p_h, \mathbf{u}_h, c_h, \mathbf{s}_h$ at t^1 are obtained from the first-order scheme introduced in Section 4.2.1.

4.3. Stability analysis

In this subsection, we proceed to prove the stability of the two fully-discrete schemes discussed in Section 4.2. We first demonstrate some useful properties of $\mathbf{D}(\mathbf{u})$ and $\mathbf{M}_e(\mathbf{u})$ whose proofs have been given in [14].

Lemma 4.1. *Given $\boldsymbol{D}(\boldsymbol{u})$ in (2.5) with $d_m > 0$, α_l and α_t are non-negative functions of x, y and are uniformly bounded, i.e. $\alpha_l(x) \leq \alpha_l^*$ and $\alpha_t(x) \leq \alpha_t^*$. Then for any $\boldsymbol{u}, \boldsymbol{v} \in R^d$,*

$$\left|\boldsymbol{D}(\boldsymbol{u})^{-1}v\right| \leq (d_m + min(\alpha_l, \alpha_t)|\boldsymbol{u}|)^{-1}|\boldsymbol{v}| \leq d_m^{-1}|\boldsymbol{v}|, \tag{4.26}$$

$$\left|\boldsymbol{D}(\boldsymbol{u})^{-1}\boldsymbol{v}\right| \geq \left(d_m + max\left(\alpha_l^*, \alpha_t^*\right)|\boldsymbol{u}|\right)^{-1}|\boldsymbol{v}|, \tag{4.27}$$

$$\left|\boldsymbol{D}(\boldsymbol{u})^{-1}-\boldsymbol{D}(\boldsymbol{v})^{-1}\right| \le d_m^{-2}\left(7\alpha_t^*+6\alpha_l^*\right)d^{3/2}\left|\boldsymbol{u}-\boldsymbol{v}\right|, \tag{4.28}$$

where d is the dimension of Ω.

Lemma 4.2. *Given* $\boldsymbol{M}_e(\boldsymbol{u})$ *in (4.6) with* $d_m > 0$. *Suppose that* α_l *and* α_t *are positive functions of* x, y *and* $0 < \alpha_{l*} \le \alpha_l(x) \le \alpha_l^*$ *and* $0 < \alpha_{t*} \le \alpha_t(x) \le \alpha_t^*$. *Then for any* $\boldsymbol{u}, \boldsymbol{v} \in R^d$,

$$\left|\boldsymbol{M}_e(\boldsymbol{u})\right| \le \left(min\left(\alpha_{l*}, \alpha_{t*}\right)\right)^{-1}, \tag{4.29}$$

$$\left|\boldsymbol{M}_e(\boldsymbol{u})-\boldsymbol{M}_e(\boldsymbol{v})\right| \le L_M\left|\boldsymbol{u}-\boldsymbol{v}\right|, \tag{4.30}$$

where $L_M = d_m^{-1} + \left(d_m min\left(\alpha_{l*}, \alpha_{t*}\right)\right)^{-1}\left(7\alpha_t^*+6\alpha_l^*\right)d^{3/2}$ *and d is the dimension of* Ω.

With the above two lemmas, we can prove the stability of the two fully-discrete LDG schemes. We start from the following theorem of ϕ_h, and the proof of Theorem 4.1 was given in [26].

Theorem 4.1. *Suppose the initial porosity* $\phi_0 > 0$, *then the approximation* ϕ_h *from the Fully-LDG(k,1) scheme satisfies*

$$\phi_0 \le \phi_h^n \le 1-\left(1-\phi_0\right)e^{-\psi T} < 1, \tag{4.31}$$

where $\psi = \frac{R}{1-\phi_0}$. *Define* $R = Ba_0 = \frac{\alpha k_c k_s a_0}{\rho_s(k_c+k_s)}$, *then we have*

$$0 \le \frac{\phi_h^{n+1}-\phi_h^n}{\tau} < R. \tag{4.32}$$

Theorem 4.2. *The discrete porosity* ϕ_h *from the Fully-LDG(k,2) scheme is bounded, i.e.,*

$$\phi_0 \le \phi_h^n \le 1-\left(1-\phi_0\right)e^{-\frac{3\psi}{2}T} < 1, \tag{4.33}$$

with

$$\tau \le \tau^* < \frac{2(1-\phi_0)}{R}, \tag{4.34}$$

where $\phi_0 > 0$ *is the initial porosity,* $\psi = \frac{R}{1-\phi_0}$ *and* τ^* *satisfies* $1-\frac{\psi\tau^*}{2} = e^{-\psi\tau^*}$. *It also holds that*

$$0 \le \frac{\phi_h^{n+1}-\phi_h^n}{\tau} < R, \tag{4.35}$$

where $R = Ba_0 = \frac{\alpha k_c k_s a_0}{\rho_s(k_c+k_s)}$, $n \ge 0$.

Proof. We use mathematical induction and assume $\phi_0 \le \phi_h^n < 1$. (4.20) can be rewritten as

$$\phi_h^{n+1} = \frac{1}{2}R\frac{1-\phi_h^{n+1}}{1-\phi_0}\bar{c}_h^{n+1,*}\tau + \frac{1}{2}R\frac{1-\phi_h^n}{1-\phi_0}\bar{c}_h^n\tau + \phi_h^n.$$

We define $\beta^{n+1,*} = R\frac{\bar{c}_h^{n+1,*}}{1-\phi_0}\tau \ge 0$ and $\beta^n = R\frac{\bar{c}_h^n}{1-\phi_0}\tau \ge 0$. Under (4.34), we have $\beta^n < 2$. Then with direct calculation, we can obtain

$$\phi_h^{n+1} = \frac{\frac{1}{2}\beta^{n+1,*}+\frac{1}{2}\beta^n+\left(1-\frac{1}{2}\beta^n\right)\phi_h^n}{1+\frac{1}{2}\beta^{n+1,*}} < 1.$$

The proof for $\phi_h^{n+1} \ge \phi_h^n \ge \phi_0$ is straightforward since the right-hand side of (4.20) is non-negative. Moreover, we have

$$\frac{\phi_h^{n+1}-\phi_h^n}{\tau} \le \frac{\psi}{2}\left(1-\phi_h^{n+1}\right)+\frac{\psi}{2}\left(1-\phi_h^n\right),$$

with $\psi = \frac{R}{1-\phi_0}$. It is easy to get

$$1-\phi_h^{n+1} \ge \frac{1-\frac{\psi\tau}{2}}{1+\frac{\psi\tau}{2}}\left(1-\phi_h^n\right),$$

leading to

$$1-\phi_h^n \ge \left(\frac{1-\frac{\psi\tau}{2}}{1+\frac{\psi\tau}{2}}\right)^n\left(1-\phi_0\right) \ge \left(\frac{e^{-\psi\tau}}{e^{\frac{\psi}{2}\tau}}\right)^n\left(1-\phi_0\right) = e^{-\frac{3\psi}{2}T}\left(1-\phi_0\right),$$

where the second step requires the condition (4.34). Hence,

$$\phi_h^n \leq 1 - e^{-\frac{3\psi}{2}T}\left(1-\phi_0\right).$$

The estimate in (4.35) is straightforward. □

Based on the above two theorems, it is easy to obtain

$$0 < F_* \leq F(\phi_h) \leq F^*, \quad 0 < \kappa_* \leq \kappa(\phi_h)^{-1} \leq \kappa^*,$$

where F_*, F^*, κ_* and κ^* are positive constants. By using Lemma 2.1, we can deduce the following result.

Lemma 4.3. *$\frac{F(\phi)}{\sqrt{\kappa(\phi)}}$ is Lipschitz continuous, i.e. there exists $C > 0$ such that*

$$\left|\frac{F(\phi_1)}{\sqrt{\kappa(\phi_1)}} - \frac{F(\phi_2)}{\sqrt{\kappa(\phi_2)}}\right| \leq C|\phi_1 - \phi_2|.$$

Proof. The Lipschitz continuity of $\frac{F(\phi)}{\sqrt{\kappa(\phi)}}$ can be obtained by

$$\begin{aligned}
\left|\frac{F(\phi_1)}{\sqrt{\kappa(\phi_1)}} - \frac{F(\phi_2)}{\sqrt{\kappa(\phi_2)}}\right| &\leq \left|\frac{F(\phi_1)}{\sqrt{\kappa(\phi_1)}} - \frac{F(\phi_2)}{\sqrt{\kappa(\phi_1)}}\right| + \left|\frac{F(\phi_2)}{\sqrt{\kappa(\phi_1)}} - \frac{F(\phi_2)}{\sqrt{\kappa(\phi_2)}}\right| \\
&\leq C\left|F(\phi_1) - F(\phi_2)\right| + C\left|\frac{1}{\sqrt{\kappa(\phi_1)}} - \frac{1}{\sqrt{\kappa(\phi_2)}}\right| \\
&\leq C\left|F(\phi_1) - F(\phi_2)\right| + C\left|\frac{1}{\sqrt{\kappa(\phi_1)}} - \frac{1}{\sqrt{\kappa(\phi_2)}}\right|\left|\frac{1}{\sqrt{\kappa(\phi_1)}} + \frac{1}{\sqrt{\kappa(\phi_2)}}\right| \\
&= C\left|F(\phi_1) - F(\phi_2)\right| + C\left|\frac{1}{\kappa(\phi_1)} - \frac{1}{\kappa(\phi_2)}\right| \\
&\leq C|\phi_1 - \phi_2|,
\end{aligned}$$

where we used the boundedness of $F(\phi_h)$ and $\kappa(\phi_h)^{-1}$. □

Then we can state the stability of the Fully-LDG(k,1) scheme.

Theorem 4.3. *The numerical approximations of the Fully-LDG(k,1) scheme satisfy*

$$\left\|p_h^n\right\|^2 + \left\|\boldsymbol{u}_h^n\right\|^2 + \tau\sum_{m=1}^{n}\left\|\boldsymbol{u}_h^m\right\|_{L^3}^3 \leq C\tau\sum_{m=1}^{n}\left\|f^{m-1}\right\|^2 + CR^2 + C\left\|p_h^0\right\|^2 + C\left\|\boldsymbol{u}_h^0\right\|^2 + C\left|\rho\mathbf{g}\right|^2, \tag{4.36}$$

$$\left\|c_h^n\right\|^2 + \tau\sum_{m=1}^{n}\left\|\boldsymbol{s}_h^m\right\|^2 \leq C\tau\sum_{m=1}^{n}\left\|f_I^{m-1}c_I^{m-1}\right\|^2 + C\left\|c_h^0\right\|^2, \tag{4.37}$$

where $C\tau \leq min(\frac{\gamma}{4}, \frac{\rho}{2}, \frac{\phi_*}{2})$, $n \geq 1$ and $R = Ba_0 = \frac{\alpha k_c k_s a_0}{\rho_s(k_c+k_s)}$.

Proof. Taking $\zeta = p_h^{n+1}$ in (4.15) and $\boldsymbol{\theta} = \mathbf{u}_h^{n+1}$ in (4.16), we obtain

$$\left(\gamma\frac{p_h^{n+1} - p_h^n}{\tau}, p_h^{n+1}\right) + \left(\frac{\phi_h^{n+1} - \phi_h^n}{\tau}, p_h^{n+1}\right) = \mathcal{L}^d\left(\mathbf{u}_h^{n+1}, p_h^{n+1}\right) + \left(f^n, p_h^{n+1}\right), \tag{4.38}$$

$$\begin{aligned}
&\left(\frac{\rho}{\phi_h^{n+1}}\frac{\mathbf{u}_h^{n+1} - \mathbf{u}_h^n}{\tau}, \mathbf{u}_h^{n+1}\right) + \left(\frac{\mu}{\kappa(\phi_h^{n+1})}\mathbf{u}_h^{n+1}, \mathbf{u}_h^{n+1}\right) + \left(\frac{\rho F\left(\phi_h^{n+1}\right)}{\sqrt{\kappa\left(\phi_h^{n+1}\right)}}\left|\mathbf{u}_h^{n+1}\right|\mathbf{u}_h^{n+1}, \mathbf{u}_h^{n+1}\right) \\
&= \mathcal{D}(p_h^{n+1}, \mathbf{u}_h^{n+1}) + \left(\rho\mathbf{g}, \mathbf{u}_h^{n+1}\right).
\end{aligned} \tag{4.39}$$

The first term in the (4.39) can be written as

$$\begin{aligned}
&\left(\frac{\rho}{\phi_h^{n+1}}\frac{\left(\mathbf{u}_h^{n+1} - \mathbf{u}_h^n\right)}{\tau}, \mathbf{u}_h^{n+1}\right) \\
&= \frac{1}{2\tau}\left(\frac{\rho}{\phi_h^{n+1}}\mathbf{u}_h^{n+1}, \mathbf{u}_h^{n+1}\right) + \frac{1}{2\tau}\left(\frac{\rho}{\phi_h^{n+1}}\left(\mathbf{u}_h^{n+1} - \mathbf{u}_h^n\right), \left(\mathbf{u}_h^{n+1} - \mathbf{u}_h^n\right)\right) - \frac{1}{2\tau}\left(\frac{\rho}{\phi_h^{n+1}}\mathbf{u}_h^n, \mathbf{u}_h^n\right)
\end{aligned}$$

$$\geq \frac{1}{2\tau}\left(\frac{\rho}{\phi_h^{n+1}}\mathbf{u}_h^{n+1},\mathbf{u}_h^{n+1}\right)+\frac{1}{2\tau}\left(\frac{\rho}{\phi_h^{n+1}}\left(\mathbf{u}_h^{n+1}-\mathbf{u}_h^{n}\right),\left(\mathbf{u}_h^{n+1}-\mathbf{u}_h^{n}\right)\right)-\frac{1}{2\tau}\left(\frac{\rho}{\phi_h^{n}}\mathbf{u}_h^{n},\mathbf{u}_h^{n}\right), \tag{4.40}$$

where we used the monotonicity of ϕ_h in the last step. Summing (4.38)–(4.39) and using (4.13) and (4.40), we have

$$\begin{aligned}
&\frac{\gamma}{2}\left(\left\|p_h^{n+1}\right\|^2+\left\|p_h^{n+1}-p_h^n\right\|^2-\left\|p_h^n\right\|^2\right)+\frac{1}{2}\left\|\sqrt{\frac{\rho}{\phi_h^{n+1}}}\mathbf{u}_h^{n+1}\right\|^2+\frac{1}{2}\left\|\sqrt{\frac{\rho}{\phi_h^{n+1}}}\left(\mathbf{u}_h^{n+1}-\mathbf{u}_h^{n}\right)\right\|^2\\
&-\frac{1}{2}\left\|\sqrt{\frac{\rho}{\phi_h^{n}}}\mathbf{u}_h^{n}\right\|^2+\tau\left\|\sqrt{\frac{\mu}{\kappa\left(\phi_h^{n+1}\right)}}\mathbf{u}_h^{n+1}\right\|^2+\tau\left\|\left(\frac{\rho F\left(\phi_h^{n+1}\right)}{\sqrt{\kappa\left(\phi_h^{n+1}\right)}}\right)^{1/3}\mathbf{u}_h^{n+1}\right\|_{L^3}^3\\
&\leq -\tau\left(\frac{\phi_h^{n+1}-\phi_h^n}{\tau},p_h^{n+1}\right)+\tau\left(f^n,p_h^{n+1}\right)+\tau\left(\rho\mathbf{g},\mathbf{u}_h^{n+1}\right)\\
&\leq \tau\left(\frac{1}{2}R^2+2\left\|p_h^n\right\|^2+2\left\|p_h^{n+1}-p_h^n\right\|^2+\frac{1}{2}\left\|f^n\right\|^2+\frac{1}{2}|\rho\mathbf{g}|^2+\left\|\mathbf{u}_h^n\right\|^2+\left\|\mathbf{u}_h^{n+1}-\mathbf{u}_h^n\right\|^2\right),
\end{aligned} \tag{4.41}$$

where the last step requires Theorem 4.1, triangle inequality and Young's inequality. Summing (4.41) over n to get

$$\begin{aligned}
&\frac{\gamma}{2}\left\|p_h^{n+1}\right\|^2+\frac{1}{2}\left\|\sqrt{\frac{\rho}{\phi_h^{n+1}}}\mathbf{u}_h^{n+1}\right\|^2+\tau\sum_{m=0}^{n}\left\|\left(\frac{\mu}{\kappa\left(\phi_h^{m+1}\right)}\right)^{1/2}\mathbf{u}_h^{m+1}\right\|^2+\tau\sum_{m=0}^{n}\left\|\left(\frac{\rho F\left(\phi_h^{m+1}\right)}{\sqrt{\kappa\left(\phi_h^{m+1}\right)}}\right)^{1/3}\mathbf{u}_h^{m+1}\right\|_{L^3}^3\\
&\leq \tau\sum_{m=0}^{n}\left(2\left\|p_h^m\right\|^2+\frac{1}{2}\left\|f^m\right\|^2+\left\|\mathbf{u}_h^m\right\|^2\right)+CR^2+C|\rho\mathbf{g}|^2+\frac{\gamma}{2}\left\|p_h^0\right\|^2+\frac{1}{2}\left\|\sqrt{\frac{\rho}{\phi_0}}\mathbf{u}_h^0\right\|^2,
\end{aligned} \tag{4.42}$$

with $\tau \leq min(\frac{\gamma}{4},\frac{\rho}{2})$. Using the discrete Gronwall's inequality, we can obtain (4.36) in Theorem 4.3.

The proof of (4.37) in Theorem 4.3 is similar to Theorem 4.5 in [26], hence we omit it. □

Now we state the stability of the Fully-LDG(k,2) scheme.

Theorem 4.4. *The approximate solutions of the Fully-LDG(k,2) scheme satisfy*

$$\begin{aligned}
&\left\|p_h^n\right\|^2+\left\|\boldsymbol{u}_h^n\right\|^2+\tau\sum_{m=2}^{n}\left\|\frac{\boldsymbol{u}_h^m+\boldsymbol{u}_h^{m-1}}{2}\right\|^2\\
&\leq CR^2+C|\rho\mathbf{g}|^2+C\tau\left\|f^0\right\|^2+C\tau\sum_{m=2}^{n}\left\|f^{m-\frac{1}{2}}\right\|^2+C\left\|p_h^0\right\|^2+C\left\|\boldsymbol{u}_h^0\right\|^2,
\end{aligned} \tag{4.43}$$

$$\left\|c_h^n\right\|^2+\tau\sum_{m=2}^{n}\left\|\frac{\boldsymbol{s}_h^m+\boldsymbol{s}_h^{m-1}}{2}\right\|^2\leq C\tau\sum_{m=2}^{n}\left\|f_I^{m-\frac{1}{2}}c_I^{m-\frac{1}{2}}\right\|^2+C\tau\left\|f_I^0c_I^0\right\|^2+C\left\|c_h^0\right\|^2, \tag{4.44}$$

where $C\tau \leq min(\frac{\gamma}{2},\frac{\phi_*}{4})$, $n>1$ and $R=Ba_0=\frac{\alpha k_c k_s a_0}{\rho_s(k_c+k_s)}$.

Proof. Taking $\zeta=\frac{p_h^{n+1}+p_h^n}{2}$ in (4.22) and $\boldsymbol{\theta}=\frac{\mathbf{u}_h^{n+1}+\mathbf{u}_h^n}{2}$ in (4.23), we obtain

$$\begin{aligned}
&\left(\gamma\frac{p_h^{n+1}-p_h^n}{\tau},\frac{p_h^{n+1}+p_h^n}{2}\right)+\left(\frac{\phi_h^{n+1}-\phi_h^n}{\tau},\frac{p_h^{n+1}+p_h^n}{2}\right)\\
&=\mathcal{L}^d\left(\frac{\mathbf{u}_h^{n+1}+\mathbf{u}_h^n}{2},\frac{p_h^{n+1}+p_h^n}{2}\right)+\left(f^{n+\frac{1}{2}},\frac{p_h^{n+1}+p_h^n}{2}\right),
\end{aligned} \tag{4.45}$$

$$\left(\frac{\rho}{\phi_h^{n+\frac{1}{2}}}\frac{\mathbf{u}_h^{n+1}-\mathbf{u}_h^n}{\tau},\frac{\mathbf{u}_h^{n+1}+\mathbf{u}_h^n}{2}\right)+\left(\frac{\rho F\left(\phi_h^{n+\frac{1}{2}}\right)}{\sqrt{\kappa\left(\phi_h^{n+\frac{1}{2}}\right)}}\left|\frac{3\mathbf{u}_h^n-\mathbf{u}_h^{n-1}}{2}\right|\frac{\mathbf{u}_h^{n+1}+\mathbf{u}_h^n}{2},\frac{\mathbf{u}_h^{n+1}+\mathbf{u}_h^n}{2}\right)$$

$$+\left(\frac{\mu}{\kappa(\phi_h^{n+\frac{1}{2}})}\frac{\mathbf{u}_h^{n+1}+\mathbf{u}_h^n}{2},\frac{\mathbf{u}_h^{n+1}+\mathbf{u}_h^n}{2}\right)=\mathcal{D}(\frac{p_h^{n+1}+p_h^n}{2},\frac{\mathbf{u}_h^{n+1}+\mathbf{u}_h^n}{2})+\left(\rho\mathbf{g},\frac{\mathbf{u}_h^{n+1}+\mathbf{u}_h^n}{2}\right). \tag{4.46}$$

With the monotonicity of ϕ_h, we obtain

$$\begin{aligned}\left(\frac{\rho}{\phi_h^{n+\frac{1}{2}}}\frac{\mathbf{u}_h^{n+1}-\mathbf{u}_h^n}{\tau},\frac{\mathbf{u}_h^{n+1}+\mathbf{u}_h^n}{2}\right)&=\frac{1}{2\tau}\left(\frac{\rho}{\phi_h^{n+\frac{1}{2}}}\mathbf{u}_h^{n+1},\mathbf{u}_h^{n+1}\right)-\frac{1}{2\tau}\left(\frac{\rho}{\phi_h^{n+\frac{1}{2}}}\mathbf{u}_h^n,\mathbf{u}_h^n\right)\\&\ge\frac{1}{2\tau}\left(\frac{\rho}{\phi_h^{n+\frac{1}{2}}}\mathbf{u}_h^{n+1},\mathbf{u}_h^{n+1}\right)-\frac{1}{2\tau}\left(\frac{\rho}{\phi_h^{n-\frac{1}{2}}}\mathbf{u}_h^n,\mathbf{u}_h^n\right).\end{aligned} \tag{4.47}$$

Summing (4.45)–(4.46), we have

$$\begin{aligned}&\frac{\gamma}{2}\left\|p_h^{n+1}\right\|^2-\frac{\gamma}{2}\left\|p_h^n\right\|^2+\frac{1}{2}\left\|\sqrt{\frac{\rho}{\phi_h^{n+\frac{1}{2}}}}\mathbf{u}_h^{n+1}\right\|^2-\frac{1}{2}\left\|\sqrt{\frac{\rho}{\phi_h^{n-\frac{1}{2}}}}\mathbf{u}_h^n\right\|^2\\&+\tau\left\|\sqrt{\frac{\mu}{\kappa(\phi_h^{n+\frac{1}{2}})}}\frac{\mathbf{u}_h^{n+1}+\mathbf{u}_h^n}{2}\right\|^2+\tau\left\|\left(\frac{\rho F\left(\phi_h^{n+\frac{1}{2}}\right)}{\sqrt{\kappa\left(\phi_h^{n+\frac{1}{2}}\right)}}\left|\frac{3\mathbf{u}_h^n-\mathbf{u}_h^{n-1}}{2}\right|\right)^{1/2}\frac{\mathbf{u}_h^{n+1}+\mathbf{u}_h^n}{2}\right\|^2\\=&-\tau\left(\frac{\phi_h^{n+1}-\phi_h^n}{\tau},\frac{p_h^{n+1}+p_h^n}{2}\right)+\tau\left(f^{n+\frac{1}{2}},\frac{p_h^{n+1}+p_h^n}{2}\right)+\tau\left(\rho\mathbf{g},\frac{\mathbf{u}_h^{n+1}+\mathbf{u}_h^n}{2}\right)\\\le&\ \tau\left(\frac{1}{2}R^2+\left\|\frac{p_h^{n+1}+p_h^n}{2}\right\|^2+\frac{1}{2}\left\|f^{n+\frac{1}{2}}\right\|^2+C\left|\rho\mathbf{g}\right|^2+\varepsilon\left\|\sqrt{\frac{\mu}{\kappa(\phi_h^{n+\frac{1}{2}})}}\frac{\mathbf{u}_h^{n+1}+\mathbf{u}_h^n}{2}\right\|^2\right)\\\le&\ \tau\left(\frac{1}{2}R^2+\frac{1}{2}\left\|p_h^{n+1}\right\|^2+\frac{1}{2}\left\|p_h^n\right\|^2+\frac{1}{2}\left\|f^{n+\frac{1}{2}}\right\|^2+C\left|\rho\mathbf{g}\right|^2+\varepsilon\left\|\sqrt{\frac{\mu}{\kappa(\phi_h^{n+\frac{1}{2}})}}\frac{\mathbf{u}_h^{n+1}+\mathbf{u}_h^n}{2}\right\|^2\right).\end{aligned} \tag{4.48}$$

Taking $\varepsilon=\frac{1}{8}$ and summing (4.48) over n leads to

$$\begin{aligned}&\frac{\gamma}{2}\left\|p_h^{n+1}\right\|^2+\frac{1}{2}\left\|\sqrt{\frac{\rho}{\phi_h^{n+\frac{1}{2}}}}\mathbf{u}_h^{n+1}\right\|^2+\frac{7\tau}{8}\sum_{m=1}^{n}\left\|\sqrt{\frac{\mu}{\kappa(\phi_h^{m+\frac{1}{2}})}}\frac{\mathbf{u}_h^{m+1}+\mathbf{u}_h^m}{2}\right\|^2\\&+\tau\sum_{m=1}^{n}\left\|\left(\frac{\rho F\left(\phi_h^{m+\frac{1}{2}}\right)}{\sqrt{\kappa\left(\phi_h^{m+\frac{1}{2}}\right)}}\left|\frac{3\mathbf{u}_h^m-\mathbf{u}_h^{m-1}}{2}\right|\right)^{1/2}\frac{\mathbf{u}_h^{m+1}+\mathbf{u}_h^m}{2}\right\|^2\\\le&\ \tau\sum_{m=1}^{n}\left\|p_h^m\right\|^2+\frac{\tau}{2}\left\|p_h^{n+1}\right\|^2+CR^2+C\left|\rho\mathbf{g}\right|^2+\frac{1}{2}\tau\sum_{m=1}^{n}\left\|f^{m+\frac{1}{2}}\right\|^2+\frac{\gamma}{2}\left\|p_h^1\right\|^2+\frac{1}{2}\left\|\sqrt{\frac{\rho}{\phi_h^{\frac{1}{2}}}}\mathbf{u}_h^1\right\|^2.\end{aligned} \tag{4.49}$$

We take $\tau\le\frac{\gamma}{2}$ to get

$$\frac{\gamma}{4}\left\|p_h^{n+1}\right\|^2+\frac{1}{2}\left\|\sqrt{\frac{\rho}{\phi_h^{n+\frac{1}{2}}}}\mathbf{u}_h^{n+1}\right\|^2+\frac{7\tau}{8}\sum_{m=1}^{n}\left\|\sqrt{\frac{\mu}{\kappa(\phi_h^{m+\frac{1}{2}})}}\frac{\mathbf{u}_h^{m+1}+\mathbf{u}_h^m}{2}\right\|^2$$

$$+\tau\sum_{m=1}^{n}\left\|\left(\frac{\rho F\left(\phi_h^{m+\frac{1}{2}}\right)}{\sqrt{\kappa\left(\phi_h^{m+\frac{1}{2}}\right)}}\left|\frac{3\mathbf{u}_h^m-\mathbf{u}_h^{m-1}}{2}\right|\right)^{1/2}\frac{\mathbf{u}_h^{m+1}+\mathbf{u}_h^m}{2}\right\|^2$$

$$\leq\tau\sum_{m=1}^{n}\left\|p_h^m\right\|^2+CR^2+C\left|\rho\mathbf{g}\right|^2+\frac{1}{2}\tau\sum_{m=1}^{n}\left\|f^{m+\frac{1}{2}}\right\|^2+\frac{\gamma}{2}\left\|p_h^1\right\|^2+\frac{1}{2}\left\|\sqrt{\frac{\rho}{\phi_h^{\frac{1}{2}}}}\mathbf{u}_h^1\right\|^2. \tag{4.50}$$

Thanks to Theorem 4.3, we have

$$\left\|p_h^1\right\|^2+\left\|\mathbf{u}_h^1\right\|^2\leq C\tau\left(\left\|f^0\right\|^2+R^2+|\rho\mathbf{g}|^2\right)+C(\left\|p_h^0\right\|^2+\left\|\mathbf{u}_h^0\right\|^2),$$

which further yields

$$\left\|p_h^{n+1}\right\|^2+\left\|\mathbf{u}_h^{n+1}\right\|^2+\tau\sum_{m=1}^{n}\left\|\frac{\mathbf{u}_h^{m+1}+\mathbf{u}_h^m}{2}\right\|^2\leq C\tau\sum_{m=1}^{n}\left(\left\|p_h^m\right\|^2+\left\|f^{m+\frac{1}{2}}\right\|^2\right)+C\left(R^2+|\rho\mathbf{g}|^2\right)$$
$$+C\tau\left\|f^0\right\|^2+C(\left\|p_h^0\right\|^2+\left\|\mathbf{u}_h^0\right\|^2). \tag{4.51}$$

Applying the discrete Gronwall's inequality, we obtain (4.43).

Next we turn to prove (4.44). Taking $v=\frac{c_h^{n+1}+c_h^n}{2}$ in (4.24) and $\mathbf{w}=\frac{\mathbf{s}_h^{n+1}+\mathbf{s}_h^n}{2}$ in (4.25), we have

$$\left(\frac{\phi_h^{n+1}c_h^{n+1}-\phi_h^nc_h^n}{\tau},\frac{c_h^{n+1}+c_h^n}{2}\right)=\mathcal{L}^d\left(\frac{\mathbf{s}_h^{n+1}+\mathbf{s}_h^n}{2},\frac{c_h^{n+1}+c_h^n}{2}\right)-\left(Aa_v\left(\phi_h^{n+\frac{1}{2}}\right)\frac{c_h^{n+1}+c_h^n}{2},\frac{c_h^{n+1}+c_h^n}{2}\right)$$
$$+\left(f_p^{n+\frac{1}{2}}\frac{c_h^{n+1}+c_h^n}{2}+f_I^{n+\frac{1}{2}}c_I^{n+\frac{1}{2}},\frac{c_h^{n+1}+c_h^n}{2}\right), \tag{4.52}$$

$$\left(\left(\phi_h^{n+\frac{1}{2}}\mathbf{D}\left(\mathbf{u}_h^{n+\frac{1}{2},M}\right)\right)^{-1}\frac{\mathbf{s}_h^{n+1}+\mathbf{s}_h^n}{2},\frac{\mathbf{s}_h^{n+1}+\mathbf{s}_h^n}{2}\right)=\left(\left(\phi_h^{n+\frac{1}{2}}\right)^{-1}\mathbf{M}_e\left(\mathbf{u}_h^{n+\frac{1}{2}}\right)\frac{c_h^{n+1}+c_h^n}{2},\frac{\mathbf{s}_h^{n+1}+\mathbf{s}_h^n}{2}\right)$$
$$+\mathcal{D}\left(\frac{c_h^{n+1}+c_h^n}{2},\frac{\mathbf{s}_h^{n+1}+\mathbf{s}_h^n}{2}\right). \tag{4.53}$$

We use (4.35) in Theorem 4.2 to obtain

$$\frac{1}{2}\left(\phi_h^{n+1}\left(c_h^{n+1}-c_h^n\right),\left(c_h^{n+1}+c_h^n\right)\right)=\frac{1}{2}\left(\phi_h^{n+1}c_h^{n+1},c_h^{n+1}\right)-\frac{1}{2}\left(\phi_h^{n+1}c_h^n,c_h^n\right)$$
$$\geq\frac{1}{2}\left(\phi_h^{n+1}c_h^{n+1},c_h^{n+1}\right)-\frac{1}{2}\left(\phi_h^nc_h^n,c_h^n\right)-\frac{\tau}{2}R\left(c_h^n,c_h^n\right). \tag{4.54}$$

Summing (4.52) and (4.53) and using (4.54), we have

$$\frac{1}{2}\left\|\sqrt{\phi_h^{n+1}}c_h^{n+1}\right\|^2-\frac{1}{2}\left\|\sqrt{\phi_h^n}c_h^n\right\|^2+\tau\left\|\left(\phi_h^{n+\frac{1}{2}}\mathbf{D}\left(\mathbf{u}_h^{n+\frac{1}{2},M}\right)\right)^{-1/2}\frac{\mathbf{s}_h^{n+1}+\mathbf{s}_h^n}{2}\right\|^2$$
$$=-\tau\left(\frac{\left(\phi_h^{n+1}-\phi_h^n\right)}{\tau}c_h^n,\frac{\left(c_h^{n+1}+c_h^n\right)}{2}\right)-\tau\left(Aa_v\left(\phi_h^{n+\frac{1}{2}}\right)\frac{c_h^{n+1}+c_h^n}{2},\frac{c_h^{n+1}+c_h^n}{2}\right)$$
$$+\tau\left(f_p^{n+\frac{1}{2}}\frac{c_h^{n+1}+c_h^n}{2}+f_I^{n+\frac{1}{2}}c_I^{n+\frac{1}{2}},\frac{c_h^{n+1}+c_h^n}{2}\right)$$
$$+\tau\left(\left(\phi_h^{n+\frac{1}{2}}\right)^{-1}\mathbf{M}_e\left(\mathbf{u}_h^{n+\frac{1}{2}}\right)\frac{c_h^{n+1}+c_h^n}{2},\frac{\mathbf{s}_h^{n+1}+\mathbf{s}_h^n}{2}\right)+\frac{\tau}{2}R\left(c_h^n,c_h^n\right)$$
$$\leq C\tau\left(\left\|\frac{c_h^{n+1}+c_h^n}{2}\right\|^2+\left\|c_h^n\right\|^2+\left\|f_I^{n+\frac{1}{2}}c_I^{n+\frac{1}{2}}\right\|^2\right)+\varepsilon\tau\left\|\left(\phi_h^{n+\frac{1}{2}}\mathbf{D}\left(\mathbf{u}_h^{n+\frac{1}{2},M}\right)\right)^{-1}\frac{\mathbf{s}_h^{n+1}+\mathbf{s}_h^n}{2}\right\|^2$$
$$\leq C\tau\left(\left\|c_h^{n+1}\right\|^2+\left\|c_h^n\right\|^2+\left\|f_I^{n+\frac{1}{2}}c_I^{n+\frac{1}{2}}\right\|^2\right)+\varepsilon\tau\left\|\left(\phi_h^{n+\frac{1}{2}}\mathbf{D}\left(\mathbf{u}_h^{n+\frac{1}{2},M}\right)\right)^{-1}\frac{\mathbf{s}_h^{n+1}+\mathbf{s}_h^n}{2}\right\|^2, \tag{4.55}$$

where the first step follows from (4.13), the second step requires the boundedness of $\mathbf{D}(\mathbf{u}_h^{n+\frac{1}{2},M})$ and $\mathbf{M}_e(\mathbf{u}_h^{n+\frac{1}{2}})$. Summing (4.55) over n and taking $C\tau \le \frac{\phi_*}{4}$ and $\varepsilon = \frac{1}{8}$, we have

$$
\begin{aligned}
&\frac{1}{4}\left\|\sqrt{\phi_h^{n+1}}c_h^{n+1}\right\|^2 + \frac{7\tau}{8}\sum_{m=1}^{n}\left\|\left(\phi_h^{m+\frac{1}{2}}\mathbf{D}\left(\mathbf{u}_h^{m+\frac{1}{2},M}\right)\right)^{-1/2}\frac{\mathbf{s}_h^{m+1}+\mathbf{s}_h^m}{2}\right\|^2 \\
&\le C\tau\sum_{m=1}^{n}\left(\left\|c_h^m\right\|^2 + \left\|f_I^{m+\frac{1}{2}}c_I^{m+\frac{1}{2}}\right\|^2\right) + \frac{1}{2}\left\|\sqrt{\phi_h^1}c_h^1\right\|^2. \qquad (4.56)
\end{aligned}
$$

By Theorem 4.3, we have

$$
\left\|c_h^1\right\|^2 \le C\tau\left\|f_I^0c_I^0\right\|^2 + C\left\|c_h^0\right\|^2,
$$

which further yields

$$
\left\|c_h^{n+1}\right\|^2 + \tau\sum_{m=1}^{n}\left\|\frac{\mathbf{s}_h^{m+1}+\mathbf{s}_h^m}{2}\right\|^2 \le C\tau\sum_{m=1}^{n}\left(\left\|c_h^m\right\|^2 + \left\|f_I^{m+\frac{1}{2}}c_I^{m+\frac{1}{2}}\right\|^2\right) + C\tau\left\|f_I^0c_I^0\right\|^2 + C\left\|c_h^0\right\|^2.
$$

Applying the discrete Gronwall's inequality, we finish the proof. □

5. Error estimate

In this paper, we use e to denote the error between the exact and numerical solutions, i.e. $e_p = p - p_h$, $e_c = c_f - c_h$, $\mathbf{e_u} = \mathbf{u} - \mathbf{u}_h$, $\mathbf{e_s} = \mathbf{s} - \mathbf{s}_h$, $e_\phi = \phi - \phi_h$. As the general treatment of the finite element methods, the errors can be split into two terms

$$
\begin{aligned}
&e_p = \xi_p - \eta_p, && \eta_p = P^+p - p, && \xi_p = P^+p - p_h,\\
&e_c = \xi_c - \eta_c, && \eta_c = P^+c_f - c_f, && \xi_c = P^+c_f - c_h,\\
&\mathbf{e_u} = \boldsymbol{\xi_u} - \boldsymbol{\eta_u}, && \boldsymbol{\eta_u} = \boldsymbol{\Pi}^-\mathbf{u} - \mathbf{u}, && \boldsymbol{\xi_u} = \boldsymbol{\Pi}^-\mathbf{u} - \mathbf{u}_h,\\
&\mathbf{e_s} = \boldsymbol{\xi_s} - \boldsymbol{\eta_s}, && \boldsymbol{\eta_s} = \boldsymbol{\Pi}^-\mathbf{s} - \mathbf{s}, && \boldsymbol{\xi_s} = \boldsymbol{\Pi}^-\mathbf{s} - \mathbf{s}_h.
\end{aligned}
$$

With direct calculation, we can show that

$$
\mathcal{L}^d(\boldsymbol{\eta_u}, v) = \mathcal{L}^d(\boldsymbol{\eta_s}, v) = 0, \quad \forall v \in Q^k(K). \qquad (5.1)
$$

From Lemma 3.2, we have the following approximation properties.

Lemma 5.1. *The projection errors satisfy, for any $n \ge 0$, the following properties*

$$
\left\|\boldsymbol{\eta}_{\mathbf{u}}^n\right\|_{L^3} + \left\|\eta_c^n\right\| + \left\|\eta_p^n\right\| + \left\|\boldsymbol{\eta}_{\mathbf{u}}^n\right\| + \left\|\boldsymbol{\eta}_{\mathbf{s}}^n\right\| \le Ch^{k+1}, \qquad (5.2)
$$

$$
\left\|\eta_c^n\right\|_\infty + \left\|\eta_p^n\right\|_\infty + \left\|\boldsymbol{\eta}_{\mathbf{u}}^n\right\|_\infty + \left\|\boldsymbol{\eta}_{\mathbf{s}}^n\right\|_\infty \le Ch^k, \qquad (5.3)
$$

$$
\left\|\eta_c^{n+1} - \eta_c^n\right\| + \left\|\eta_p^{n+1} - \eta_p^n\right\| \le Ch^{k+1}\tau. \qquad (5.4)
$$

For the special projections given above, we will demonstrate the following lemma by the standard approximation theory [28].

Lemma 5.2. *We choose the initial solution as the way in (4.19), then we have*

$$
\|c_f(x,y,0) - c_h(x,y,0)\| + \|p(x,y,0) - p_h(x,y,0)\| + \|\boldsymbol{u}(x,y,0) - \boldsymbol{u}_h(x,y,0)\| \le Ch^{k+1}.
$$

5.1. The main result of the Fully-LDG(k,1) scheme

We first present some results of ϕ_h, c_h and $\mathbf{s}_h$ of the Fully-LDG(k,1) and we refer the readers to [26] for more details.

Lemma 5.3. *The ϕ_h of the Fully-LDG(k,1) satisfies the following estimates*

$$
\begin{aligned}
&\frac{1}{2}\left\|e_\phi^{n+1}\right\|^2 + \frac{1}{2}\left\|e_\phi^{n+1} - e_\phi^n\right\|^2 - \frac{1}{2}\left\|e_\phi^n\right\|^2 \\
&\le C\tau\left(\left\|e_\phi^{n+1}\right\| + \left\|\xi_c^n\right\| + \left\|\eta_c^n\right\| + \tau\right)\left\|e_\phi^{n+1}\right\| \\
&\le C\tau\left(\left\|e_\phi^{n+1} - e_\phi^n\right\|^2 + \left\|e_\phi^n\right\|^2 + \left\|\xi_c^n\right\|^2 + h^{2k+2} + \tau^2\right), \qquad (5.5)
\end{aligned}
$$

and

$$
\left\|\frac{e_\phi^{n+1} - e_\phi^n}{\tau}\right\| \le C\left(\left\|e_\phi^{n+1}\right\| + \left\|\xi_c^n\right\| + h^{k+1} + \tau\right). \qquad (5.6)
$$

Lemma 5.4. *The c_h and $\boldsymbol{s}_h$ of the Fully-LDG(k,1) satisfy the following estimate*

$$\begin{aligned}
&\frac{1}{2}\left\|\sqrt{\phi_h^{n+1}}\xi_c^{n+1}\right\|^2+\frac{1}{2}\left\|\sqrt{\phi_h^{n+1}}(\xi_c^{n+1}-\xi_c^n)\right\|^2-\frac{1}{2}\left\|\sqrt{\phi_h^n}\xi_c^n\right\|^2+\tau\left\|\left(\phi_h^{n+1}\boldsymbol{D}(\boldsymbol{u}_h^{n+1,M})\right)^{-1/2}\boldsymbol{\xi}_{\boldsymbol{s}}^{n+1}\right\|^2\\
&\le C\tau\left(h^{k+1}+\|e_\phi^{n+1}\|+\|e_\phi^n\|+\|\xi_c^n\|+\tau\right)\|\xi_c^{n+1}\|\\
&\quad+C\tau\left(\|\boldsymbol{\xi}_{\boldsymbol{u}}^{n+1}\|+\|\xi_c^{n+1}\|+\|e_\phi^{n+1}\|+h^{k+1}\right)\|\boldsymbol{\xi}_{\boldsymbol{s}}^{n+1}\|+\frac{1}{2}\tau R\left(\xi_c^n,\xi_c^n\right)\\
&\le C\tau\left(\left\|e_\phi^{n+1}-e_\phi^n\right\|^2+\left\|e_\phi^n\right\|^2+\left\|\xi_c^n\right\|^2+\left\|\xi_c^{n+1}-\xi_c^n\right\|^2+\left\|\boldsymbol{\xi}_{\boldsymbol{u}}^{n+1}-\boldsymbol{\xi}_{\boldsymbol{u}}^n\right\|^2+\left\|\boldsymbol{\xi}_{\boldsymbol{u}}^n\right\|^2+h^{2k+2}+\tau^2\right)\\
&\quad+\varepsilon\tau\left\|\left(\phi_h^{n+1}\boldsymbol{D}(\boldsymbol{u}_h^{n+1,M})\right)^{-1/2}\boldsymbol{\xi}_{\boldsymbol{s}}^{n+1}\right\|^2.
\end{aligned}\tag{5.7}$$

Now we state the main theorem of the Fully-LDG(k,1) scheme.

Theorem 5.1. *Let $c_f\in L^\infty(0,T;H^{k+3})$, $\boldsymbol{s}\in L^\infty(0,T;(H^{k+2})^2)$, $\boldsymbol{u}\in L^\infty(0,T;(H^{k+2})^2)$, $\phi\in L^\infty(0,T;H^{k+3})$ be the exact solutions of problem (4.1)–(4.5), and let c_h, $\boldsymbol{s}_h$, $\boldsymbol{u}_h$, ϕ_h, p_h be the numerical solutions of Fully-LDG(k,1) scheme with initial discretization given as (4.19). If the finite element space is made up of piecewise tensor product polynomials of degree at most k and assume the time step τ satisfies*

$$C\tau\le min(\frac{1}{2},\frac{\gamma}{4},\frac{\rho}{2},\frac{\phi_*}{2}),$$

then the Fully-LDG(k,1) scheme satisfies

$$\|\xi_c^n\|^2+\|\xi_p^n\|^2+\|e_\phi^n\|^2+\|\boldsymbol{\xi}_{\boldsymbol{u}}^n\|^2+\tau\sum_{m=1}^n\|\boldsymbol{\xi}_{\boldsymbol{u}}^m\|_{L^3}^3+\tau\sum_{m=1}^n\|\boldsymbol{\xi}_{\boldsymbol{s}}^m\|^2\le C\left(h^{2k+2}+\tau^2\right),\quad\forall n\ge 1,\tag{5.8}$$

which further yields the optimal error estimate

$$\|e_c^n\|^2+\|e_p^n\|^2+\|e_\phi^n\|^2+\|\boldsymbol{e}_{\boldsymbol{u}}^n\|^2+\tau\sum_{m=1}^n\|\boldsymbol{e}_{\boldsymbol{u}}^m\|_{L_3}^3+\tau\sum_{m=1}^n\|\boldsymbol{e}_{\boldsymbol{s}}^m\|^2\le C\left(h^{2k+2}+\tau^2\right),\quad\forall n\ge 1.\tag{5.9}$$

Proof. Based on Lemmas 5.3 and 5.4, we only need to split the proof into two steps.
Step 1. The exact solutions satisfy the following variational forms

$$\left(\gamma\frac{p^{n+1}-p^n}{\tau},\zeta\right)+\left(\frac{\phi^{n+1}-\phi^n}{\tau},\zeta\right)=\mathcal{L}^d\left(\mathbf{u}^{n+1},\zeta\right)+\left(f^n,\zeta\right)+\left(\varsigma_1^n,\zeta\right),\tag{5.10}$$

$$\begin{aligned}
&\left(\frac{\rho}{\phi^{n+1}}\frac{\mathbf{u}^{n+1}-\mathbf{u}^n}{\tau},\boldsymbol{\theta}\right)+\left(\frac{\mu}{\kappa(\phi^{n+1})}\mathbf{u}^{n+1},\boldsymbol{\theta}\right)+\left(\frac{\rho F\left(\phi^{n+1}\right)}{\sqrt{\kappa\left(\phi^{n+1}\right)}}\left|\mathbf{u}^{n+1}\right|\mathbf{u}^{n+1},\boldsymbol{\theta}\right)\\
&=\mathcal{D}(p^{n+1},\boldsymbol{\theta})+(\rho\mathbf{g},\boldsymbol{\theta})+\left(\varsigma_2^n,\boldsymbol{\theta}\right),
\end{aligned}\tag{5.11}$$

$$\left(\frac{\phi^{n+1}c_f^{n+1}-\phi^n c_f^n}{\tau},v\right)=\mathcal{L}^d\left(\mathbf{s}^{n+1},v\right)-\left(Aa_v\left(\phi^n\right)c_f^n,v\right)+\left(f_p^n c_f^n+f_I^n c_I^n,v\right)+\left(\varsigma_3^n,v\right),\tag{5.12}$$

$$\left(\left(\phi^{n+1}\mathbf{D}(\mathbf{u}^{n+1})\right)^{-1}\mathbf{s}^{n+1},\mathbf{w}\right)=\left(\left(\phi^{n+1}\right)^{-1}\mathbf{M}_e\left(\mathbf{u}^{n+1}\right)c_f^{n+1},\mathbf{w}\right)+\mathcal{D}\left(c_f^{n+1},\mathbf{w}\right),\tag{5.13}$$

$$\frac{\phi^{n+1}-\phi^n}{\tau}=Ba_v\left(\phi^{n+1}\right)c_f^n+\varsigma_4^n,\tag{5.14}$$

where $\zeta,v\in W_h^k$ and $\boldsymbol{\theta},\mathbf{w}\in\mathbf{W}_h^k$. Here ς_i^n, $i=1,2,3,4$ are local truncation errors satisfying

$$\left\|\varsigma_i^n\right\|\le C\tau,\quad i=1,2,3,4,\quad\forall n\ge 0.\tag{5.15}$$

Subtracting (5.10)–(5.14) from (4.14)–(4.18), we get the following error equations

$$\left(\gamma\frac{e_p^{n+1}-e_p^n}{\tau},\zeta\right)+\left(\frac{e_\phi^{n+1}-e_\phi^n}{\tau},\zeta\right)=\mathcal{L}^d\left(\mathbf{e}_{\mathbf{u}}^{n+1},\zeta\right)+\left(\varsigma_1^n,\zeta\right),\tag{5.16}$$

$$\left(\frac{\rho}{\phi^{n+1}}\frac{\mathbf{u}^{n+1}-\mathbf{u}^n}{\tau}-\frac{\rho}{\phi_h^{n+1}}\frac{\mathbf{u}_h^{n+1}-\mathbf{u}_h^n}{\tau},\boldsymbol{\theta}\right)+\left(\frac{\mu}{\kappa\left(\phi^{n+1}\right)}\mathbf{u}^{n+1}-\frac{\mu}{\kappa\left(\phi_h^{n+1}\right)}\mathbf{u}_h^{n+1},\boldsymbol{\theta}\right)$$

$$+\left(\frac{\rho F(\phi^{n+1})}{\sqrt{\kappa(\phi^{n+1})}}\left|\mathbf{u}^{n+1}\right|\mathbf{u}^{n+1}-\frac{\rho F(\phi_h^{n+1})}{\sqrt{\kappa(\phi_h^{n+1})}}\left|\mathbf{u}_h^{n+1}\right|\mathbf{u}_h^{n+1},\boldsymbol{\theta}\right)=\mathcal{D}\left(e_p^{n+1},\boldsymbol{\theta}\right)+\left(\varsigma_2^n,\boldsymbol{\theta}\right),\tag{5.17}$$

$$\begin{aligned}&\left(\frac{\phi^{n+1}c_f^{n+1}-\phi^n c_f^n-\left(\phi_h^{n+1}c_h^{n+1}-\phi_h^n c_h^n\right)}{\tau},v\right)\\&=\mathcal{L}^d\left(\mathbf{e}_\mathbf{s}^{n+1},v\right)-\left(Aa_v\left(\phi^n\right)c_f^n-Aa_v\left(\phi_h^n\right)c_h^n,v\right)+\left(f_p^n e_c^n,v\right)+\left(\varsigma_3^n,v\right),\end{aligned}\tag{5.18}$$

$$\begin{aligned}&\left(\left(\phi^{n+1}\mathbf{D}(\mathbf{u}^{n+1})\right)^{-1}\mathbf{s}^{n+1}-\left(\phi_h^{n+1}\mathbf{D}(\mathbf{u}_h^{n+1,M})\right)^{-1}\mathbf{s}_h^{n+1},\mathbf{w}\right)\\&=\left(\left(\phi^{n+1}\right)^{-1}\mathbf{M}_e\left(\mathbf{u}^{n+1}\right)c_f^{n+1}-\left(\phi_h^{n+1}\right)^{-1}\mathbf{M}_e\left(\mathbf{u}_h^{n+1}\right)c_h^{n+1},\mathbf{w}\right)+\mathcal{D}\left(e_c^{n+1},\mathbf{w}\right),\end{aligned}\tag{5.19}$$

$$\frac{e_\phi^{n+1}-e_\phi^n}{\tau}=Ba_v\left(\phi^{n+1}\right)c_f^n-Ba_v\left(\phi_h^{n+1}\right)\bar{c}_h^n+\varsigma_4^n.\tag{5.20}$$

Step 2. We take $\zeta=\xi_p^{n+1}$ in (5.16) and $\boldsymbol{\theta}=\boldsymbol{\xi}_\mathbf{u}^{n+1}$ in (5.17), and sum up these two equations to get

$$\begin{aligned}&\left(\gamma\frac{\xi_p^{n+1}-\xi_p^n}{\tau},\xi_p^{n+1}\right)+\left(\frac{\mu}{\kappa\left(\phi_h^{n+1}\right)}\boldsymbol{\xi}_\mathbf{u}^{n+1},\boldsymbol{\xi}_\mathbf{u}^{n+1}\right)+\left(\frac{\rho}{\phi_h^{n+1}}\frac{\boldsymbol{\xi}_\mathbf{u}^{n+1}-\boldsymbol{\xi}_\mathbf{u}^n}{\tau},\boldsymbol{\xi}_\mathbf{u}^{n+1}\right)\\&+\left(\frac{\rho F\left(\phi_h^{n+1}\right)}{\sqrt{\kappa\left(\phi_h^{n+1}\right)}}\left(\left|\mathbf{u}^{n+1}\right|\mathbf{u}^{n+1}-\left|\mathbf{u}_h^{n+1}\right|\mathbf{u}_h^{n+1}\right),\boldsymbol{\xi}_\mathbf{u}^{n+1}\right)=\sum_{i=1}^{6}T_i,\end{aligned}\tag{5.21}$$

where

$$\begin{aligned}T_1&=\left(\gamma\frac{\eta_p^{n+1}-\eta_p^n}{\tau},\xi_p^{n+1}\right)-\left(\frac{e_\phi^{n+1}-e_\phi^n}{\tau},\xi_p^{n+1}\right),\\T_2&=\left(\frac{\mu}{\kappa\left(\phi_h^{n+1}\right)}\boldsymbol{\eta}_\mathbf{u}^{n+1},\boldsymbol{\xi}_\mathbf{u}^{n+1}\right)+\left(\left(\frac{\mu}{\kappa\left(\phi_h^{n+1}\right)}-\frac{\mu}{\kappa\left(\phi^{n+1}\right)}\right)\mathbf{u}^{n+1},\boldsymbol{\xi}_\mathbf{u}^{n+1}\right),\\T_3&=-\mathcal{D}\left(\eta_p^{n+1},\boldsymbol{\xi}_\mathbf{u}^{n+1}\right),\\T_4&=\left(\varsigma_1^n,\xi_p^{n+1}\right)+\left(\varsigma_2^n,\boldsymbol{\xi}_\mathbf{u}^{n+1}\right),\\T_5&=\left(\frac{\rho}{\phi_h^{n+1}}\frac{\boldsymbol{\eta}_\mathbf{u}^{n+1}-\boldsymbol{\eta}_\mathbf{u}^n}{\tau},\boldsymbol{\xi}_\mathbf{u}^{n+1}\right)+\left(\left(\frac{\rho}{\phi_h^{n+1}}-\frac{\rho}{\phi^{n+1}}\right)\frac{\mathbf{u}^{n+1}-\mathbf{u}^n}{\tau},\boldsymbol{\xi}_\mathbf{u}^{n+1}\right),\\T_6&=\left(\left(\frac{\rho F\left(\phi_h^{n+1}\right)}{\sqrt{\kappa\left(\phi_h^{n+1}\right)}}-\frac{\rho F\left(\phi^{n+1}\right)}{\sqrt{\kappa\left(\phi^{n+1}\right)}}\right)\left|\mathbf{u}^{n+1}\right|\mathbf{u}^{n+1},\boldsymbol{\xi}_\mathbf{u}^{n+1}\right).\end{aligned}$$

We first estimate the last term on the left-hand side of the above equation,

$$\begin{aligned}&\left(\frac{\rho F\left(\phi_h^{n+1}\right)}{\sqrt{\kappa\left(\phi_h^{n+1}\right)}}\left(\left|\mathbf{u}^{n+1}\right|\mathbf{u}^{n+1}-\left|\mathbf{u}_h^{n+1}\right|\mathbf{u}_h^{n+1}\right),\boldsymbol{\xi}_\mathbf{u}^{n+1}\right)\\&=\left(\frac{\rho F\left(\phi_h^{n+1}\right)}{\sqrt{\kappa\left(\phi_h^{n+1}\right)}}\left(\left|\mathbf{u}^{n+1}\right|-\left|\mathbf{u}_h^{n+1}\right|\right)\mathbf{u}^{n+1},\boldsymbol{\xi}_\mathbf{u}^{n+1}\right)+\left(\frac{\rho F\left(\phi_h^{n+1}\right)}{\sqrt{\kappa\left(\phi_h^{n+1}\right)}}\left|\mathbf{u}^{n+1}-\mathbf{u}_h^{n+1}\right|\left(\mathbf{u}^{n+1}-\mathbf{u}_h^{n+1}\right),\boldsymbol{\xi}_\mathbf{u}^{n+1}\right)\\&\quad+\left(\frac{\rho F\left(\phi_h^{n+1}\right)}{\sqrt{\kappa\left(\phi_h^{n+1}\right)}}\left(\left|\mathbf{u}_h^{n+1}\right|-\left|\mathbf{u}^{n+1}-\mathbf{u}_h^{n+1}\right|\right)\left(\mathbf{u}^{n+1}-\mathbf{u}_h^{n+1}\right),\boldsymbol{\xi}_\mathbf{u}^{n+1}\right)\\&:=H_1+H_2+H_3.\end{aligned}$$

Using hypothesis 3, the boundedness of ϕ_h^{n+1} and the triangle inequality $\| w\,|-|\,w-v\|\le|v|$, we have

$$|H_1|+|H_3|\le C\left(\left\|\boldsymbol{\xi}_\mathbf{u}^{n+1}\right\|+h^{k+1}\right)\left\|\boldsymbol{\xi}_\mathbf{u}^{n+1}\right\|.$$

Next, we estimate H_2. We have

$$\begin{aligned}
H_2 &= \left(\frac{\rho F\left(\phi_h^{n+1}\right)}{\sqrt{\kappa\left(\phi_h^{n+1}\right)}} \left|\boldsymbol{\xi}_{\mathbf{u}}^{n+1}\right| \boldsymbol{\xi}_{\mathbf{u}}^{n+1}, \boldsymbol{\xi}_{\mathbf{u}}^{n+1} \right) + \left(\frac{\rho F\left(\phi_h^{n+1}\right)}{\sqrt{\kappa\left(\phi_h^{n+1}\right)}} \left(\left|\mathbf{e}_{\mathbf{u}}^{n+1}\right| - \left|\boldsymbol{\xi}_{\mathbf{u}}^{n+1}\right|\right) \boldsymbol{\xi}_{\mathbf{u}}^{n+1}, \boldsymbol{\xi}_{\mathbf{u}}^{n+1} \right) \\
&\quad - \left(\frac{\rho F\left(\phi_h^{n+1}\right)}{\sqrt{\kappa\left(\phi_h^{n+1}\right)}} \left|\mathbf{e}_{\mathbf{u}}^{n+1}\right| \boldsymbol{\eta}_{\mathbf{u}}^{n+1}, \boldsymbol{\xi}_{\mathbf{u}}^{n+1} \right) \\
&\geq \left\| \left(\frac{\rho F\left(\phi_h^{n+1}\right)}{\sqrt{\kappa\left(\phi_h^{n+1}\right)}} \right)^{1/3} \boldsymbol{\xi}_{\mathbf{u}}^{n+1} \right\|_{L^3}^3 - 2 \left\| \left(\frac{\rho F\left(\phi_h^{n+1}\right)}{\sqrt{\kappa\left(\phi_h^{n+1}\right)}} \right)^{1/3} \boldsymbol{\eta}_{\mathbf{u}}^{n+1} \right\|_{L^3} \left\| \left(\frac{\rho F\left(\phi_h^{n+1}\right)}{\sqrt{\kappa\left(\phi_h^{n+1}\right)}} \right)^{1/3} \boldsymbol{\xi}_{\mathbf{u}}^{n+1} \right\|_{L^3}^2 \\
&\quad - \left\| \left(\frac{\rho F\left(\phi_h^{n+1}\right)}{\sqrt{\kappa\left(\phi_h^{n+1}\right)}} \right)^{1/3} \boldsymbol{\xi}_{\mathbf{u}}^{n+1} \right\|_{L^3} \left\| \left(\frac{\rho F\left(\phi_h^{n+1}\right)}{\sqrt{\kappa\left(\phi_h^{n+1}\right)}} \right)^{1/3} \boldsymbol{\eta}_{\mathbf{u}}^{n+1} \right\|_{L^3}^2 \\
&\geq \frac{1}{2} \left\| \left(\frac{\rho F\left(\phi_h^{n+1}\right)}{\sqrt{\kappa\left(\phi_h^{n+1}\right)}} \right)^{1/3} \boldsymbol{\xi}_{\mathbf{u}}^{n+1} \right\|_{L^3}^3 - C \left\|\boldsymbol{\eta}_{\mathbf{u}}^{n+1}\right\|_{L^3}^3 .
\end{aligned}$$

Now we estimate $T_i (i = 1, 2, 3, 4, 5, 6)$ term by term. We estimate T_1 by Schwarz inequality, Lemma 5.1 and (5.6),

$$T_1 \leq C \left(\left\|e_\phi^{n+1}\right\| + \left\|\xi_c^n\right\| + h^{k+1} + \tau \right) \left\|\xi_p^{n+1}\right\| .$$

Using hypothesis 3 and Lemma 2.1 to obtain

$$T_2 \leq C \left(h^{k+1} + \left\|e_\phi^{n+1}\right\| \right) \left\|\boldsymbol{\xi}_{\mathbf{u}}^{n+1}\right\| .$$

The estimate of T_3 follows from Lemma 3.3 and

$$T_3 \leq C h^{k+1} \left\|p^{n+1}\right\|_{k+2} \left\|\boldsymbol{\xi}_{\mathbf{u}}^{n+1}\right\| .$$

For T_4, we apply Schwarz inequality to get

$$T_4 \leq C\tau \left\|\xi_p^{n+1}\right\| + C\tau \left\|\boldsymbol{\xi}_{\mathbf{u}}^{n+1}\right\| .$$

The estimate of T_5 requires hypothesis 3, the boundedness of ϕ_h^{n+1} and Lemma 5.1,

$$T_5 \leq C \left(\left\|e_\phi^{n+1}\right\| + h^{k+1} \right) \left\|\boldsymbol{\xi}_{\mathbf{u}}^{n+1}\right\| .$$

Finally, we apply hypothesis 3 and Lemma 4.3 to estimate T_6,

$$T_6 \leq C \left\|e_\phi^{n+1}\right\| \left\|\boldsymbol{\xi}_{\mathbf{u}}^{n+1}\right\| .$$

Substituting all the above estimates into (5.21), with the monotonicity of ϕ_h, we have

$$\begin{aligned}
&\frac{\gamma}{2} \left\|\xi_p^{n+1}\right\|^2 + \frac{\gamma}{2} \left\|\xi_p^{n+1} - \xi_p^n\right\|^2 - \frac{\gamma}{2} \left\|\xi_p^n\right\|^2 + \tau \left\| \sqrt{\frac{\mu}{\kappa\left(\phi_h^{n+1}\right)}} \boldsymbol{\xi}_{\mathbf{u}}^{n+1} \right\|^2 \\
&+ \frac{1}{2} \left\| \sqrt{\frac{\rho}{\phi_h^{n+1}}} \boldsymbol{\xi}_{\mathbf{u}}^{n+1} \right\|^2 + \frac{1}{2} \left\| \sqrt{\frac{\rho}{\phi_h^{n+1}}} \left(\boldsymbol{\xi}_{\mathbf{u}}^{n+1} - \boldsymbol{\xi}_{\mathbf{u}}^n\right) \right\|^2 - \frac{1}{2} \left\| \sqrt{\frac{\rho}{\phi_h^n}} \boldsymbol{\xi}_{\mathbf{u}}^n \right\|^2 + \frac{1}{2}\tau \left\| \left(\frac{\rho F\left(\phi_h^{n+1}\right)}{\sqrt{\kappa\left(\phi_h^{n+1}\right)}} \right)^{1/3} \boldsymbol{\xi}_{\mathbf{u}}^{n+1} \right\|_{L^3}^3 \\
&\leq C\tau \left(\left\|e_\phi^{n+1}\right\| + \left\|\xi_c^n\right\| + h^{k+1} + \tau \right) \left\|\xi_p^{n+1}\right\| + C\tau \left(\left\|\boldsymbol{\xi}_{\mathbf{u}}^{n+1}\right\| + \left\|e_\phi^{n+1}\right\| + h^{k+1} + \tau \right) \left\|\boldsymbol{\xi}_{\mathbf{u}}^{n+1}\right\| + C\tau \left\|\boldsymbol{\eta}_{\mathbf{u}}^{n+1}\right\|_{L^3}^3 \\
&\leq C\tau \left(\left\|e_\phi^{n+1} - e_\phi^n\right\|^2 + \left\|e_\phi^n\right\|^2 + \left\|\xi_c^n\right\|^2 + \left\|\xi_p^{n+1} - \xi_p^n\right\|^2 + \left\|\xi_p^n\right\|^2 + \left\|\boldsymbol{\xi}_{\mathbf{u}}^{n+1} - \boldsymbol{\xi}_{\mathbf{u}}^n\right\|^2 + \left\|\boldsymbol{\xi}_{\mathbf{u}}^n\right\|^2 + h^{2k+2} + \tau^2 \right),
\end{aligned} \tag{5.22}$$

where the last step follows from Young's inequality.

Under the condition $C\tau \leq min(\frac{1}{2}, \frac{\gamma}{4}, \frac{\rho}{2}, \frac{\phi_*}{2})$, combining (5.5), (5.7) and (5.22), and summing it over n, we can obtain (5.8) by discrete Gronwall's inequality, which further yields (5.9) by standard approximation results. □

5.2. The main result of the Fully-LDG(k,2) scheme

Since the Fully-LDG(k,2) scheme contains more than one time levels, the following lemma is helpful in preparing the initial solutions.

Lemma 5.5. *With the initial solution given in (4.19), the error estimates of the solutions at the first time level t^1 satisfy*

$$\left\|e_\phi^1\right\|^2+\left\|\xi_p^1\right\|^2+\left\|\boldsymbol{\xi}_{\boldsymbol{u}}^1\right\|^2+\left\|\xi_c^1\right\|^2+\tau\left\|\boldsymbol{\xi}_{\boldsymbol{u}}^1\right\|_{L^3}^3+\tau\left\|\boldsymbol{\xi}_{\boldsymbol{s}}^1\right\|^2\leq C(h^{2k+2}+\tau^4). \tag{5.23}$$

Proof. Combining (5.5), (5.7) and (5.22) with $n=0$ leads to

$$\begin{aligned}
&\frac{1}{2}\left\|e_\phi^1\right\|^2+\frac{\gamma}{2}\left\|\xi_p^1\right\|^2+\frac{1}{2}\left\|\sqrt{\frac{\rho}{\phi_h^1}}\boldsymbol{\xi}_{\mathbf{u}}^1\right\|^2+\frac{1}{2}\left\|\sqrt{\phi_h^1}\xi_c^1\right\|^2+\tau\left\|\sqrt{\frac{\mu}{\kappa\left(\phi_h^1\right)}}\boldsymbol{\xi}_{\mathbf{u}}^1\right\|^2\\
&+\frac{1}{2}\tau\left\|\left(\frac{\rho F(\phi_h^1)}{\sqrt{\kappa(\phi_h^1)}}\right)^{1/3}\boldsymbol{\xi}_{\mathbf{u}}^1\right\|_{L^3}^3+\tau\left\|\left(\phi_h^1\mathbf{D}(\mathbf{u}_h^{1,M})\right)^{-1/2}\boldsymbol{\xi}_{\mathbf{s}}^1\right\|^2\\
\leq{}& C\tau\left(\left\|e_\phi^1\right\|+h^{k+1}+\tau\right)\left\|e_\phi^1\right\|+C\tau\left(\left\|e_\phi^1\right\|+\left\|\boldsymbol{\xi}_{\mathbf{u}}^1\right\|+h^{k+1}+\tau\right)\left\|\boldsymbol{\xi}_{\mathbf{u}}^1\right\|\\
&+C\tau\left(\left\|e_\phi^1\right\|+h^{k+1}+\tau\right)\left\|\xi_c^1\right\|+C\tau\left(\left\|e_\phi^1\right\|+h^{k+1}+\tau\right)\left\|\xi_p^1\right\|\\
&+C\tau\left(\left\|e_\phi^1\right\|+\left\|\xi_c^1\right\|+\left\|\boldsymbol{\xi}_{\mathbf{u}}^1\right\|+h^{k+1}\right)\left\|\boldsymbol{\xi}_{\mathbf{s}}^1\right\|+C\tau h^{2k+2}\\
\leq{}& C\tau\left(\left\|e_\phi^1\right\|^2+\left\|\xi_c^1\right\|^2+\left\|\xi_p^1\right\|^2+\left\|\boldsymbol{\xi}_{\mathbf{u}}^1\right\|^2\right)+\varepsilon\tau\left\|\boldsymbol{\xi}_{\mathbf{s}}^1\right\|^2\\
&+\varepsilon\left(\left\|e_\phi^1\right\|^2+\left\|\xi_c^1\right\|^2+\left\|\xi_p^1\right\|^2+\left\|\boldsymbol{\xi}_{\mathbf{u}}^1\right\|^2\right)+C\tau h^{2k+2}+C\tau^4,
\end{aligned}$$

where τ and ε are small enough. Then we get (5.23). □

Now we state the main theorem of the Fully-LDG(k,2) scheme.

Theorem 5.2. *Let $c_f\in L^\infty(0,T;H^{k+3})$, $\boldsymbol{s}\in L^\infty(0,T;(H^{k+2})^2)$, $\boldsymbol{u}\in L^\infty(0,T;(H^{k+2})^2)$, $\phi\in L^\infty(0,T;H^{k+3})$ be the exact solutions of (4.1)–(4.5), and let c_h, $\boldsymbol{s}_h$, $\boldsymbol{u}_h$, ϕ_h, p_h be the numerical solutions of the second-order time integration scheme with initial discretization given as (4.19). If the finite element space is made up of piecewise tensor product polynomials of degree at most k and assume*

$$C\tau\leq min(\frac{1}{4},\frac{\gamma}{4},\frac{\rho}{4},\frac{\phi_*}{4}),$$

then the Fully-LDG(k,2) scheme satisfies

$$\|\xi_c^n\|^2+\|\xi_p^n\|^2+\|e_\phi^n\|^2+\|\boldsymbol{\xi}_{\boldsymbol{u}}^n\|^2+\tau\sum_{m=2}^{n}\|\frac{\boldsymbol{\xi}_{\boldsymbol{u}}^m+\boldsymbol{\xi}_{\boldsymbol{u}}^{m-1}}{2}\|^2+\tau\sum_{m=2}^{n}\|\frac{\boldsymbol{\xi}_{\boldsymbol{s}}^m+\boldsymbol{\xi}_{\boldsymbol{s}}^{m-1}}{2}\|^2\leq C\left(h^{2k+2}+\tau^4\right),\forall n>1, \tag{5.24}$$

which further yields the optimal error estimate

$$\|e_c^n\|^2+\|e_p^n\|^2+\|e_\phi^n\|^2+\|\boldsymbol{e}_{\boldsymbol{u}}^n\|^2+\tau\sum_{m=2}^{n}\|\frac{\boldsymbol{e}_{\boldsymbol{u}}^m+\boldsymbol{e}_{\boldsymbol{u}}^{m-1}}{2}\|^2+\tau\sum_{m=2}^{n}\|\frac{\boldsymbol{e}_{\boldsymbol{s}}^m+\boldsymbol{e}_{\boldsymbol{s}}^{m-1}}{2}\|^2\leq C\left(h^{2k+2}+\tau^4\right),\forall n>1. \tag{5.25}$$

Proof. We split the proof into four steps.
Step 1. The exact solutions satisfy, for any $n\geq 1$, the following forms

$$\left(\gamma\frac{p^{n+1}-p^n}{\tau},\zeta\right)+\left(\frac{\phi^{n+1}-\phi^n}{\tau},\zeta\right)=\mathcal{L}^d\left(\frac{\mathbf{u}^{n+1}+\mathbf{u}^n}{2},\zeta\right)+\left(f^{n+\frac{1}{2}},\zeta\right)+\left(\varsigma_1^{n+\frac{1}{2}},\zeta\right), \tag{5.26}$$

$$\begin{aligned}
&\left(\frac{\rho}{\phi^{n+\frac{1}{2}}}\frac{\mathbf{u}^{n+1}-\mathbf{u}^n}{\tau},\boldsymbol{\theta}\right)+\left(\frac{\rho F\left(\phi^{n+\frac{1}{2}}\right)}{\sqrt{\kappa\left(\phi^{n+\frac{1}{2}}\right)}}\left|\frac{3\mathbf{u}^n-\mathbf{u}^{n-1}}{2}\right|\frac{\mathbf{u}^{n+1}+\mathbf{u}^n}{2},\boldsymbol{\theta}\right)\\
={}&-\left(\frac{\mu}{\kappa\left(\phi^{n+\frac{1}{2}}\right)}\frac{\mathbf{u}^{n+1}+\mathbf{u}^{\mathbf{n}}}{2},\boldsymbol{\theta}\right)+\mathcal{D}\left(\frac{p^{n+1}+p^n}{2},\boldsymbol{\theta}\right)+(\rho\mathbf{g},\boldsymbol{\theta})+\left(\varsigma_2^{n+\frac{1}{2}},\boldsymbol{\theta}\right),
\end{aligned} \tag{5.27}$$

$$\begin{aligned}
\left(\frac{\phi^{n+1}c_f^{n+1}-\phi^n c_f^n}{\tau},v\right)={}&\mathcal{L}^d\left(\frac{\mathbf{s}^{n+1}+\mathbf{s}^n}{2},v\right)-\left(Aa_v\left(\phi^{n+\frac{1}{2}}\right)\frac{c_f^{n+1}+c_f^n}{2},v\right)\\
&+\left(f_p^{n+\frac{1}{2}}\frac{c_f^{n+1}+c_f^n}{2}+f_I^{n+\frac{1}{2}}c_I^{n+\frac{1}{2}},v\right)+\left(\varsigma_3^{n+\frac{1}{2}},v\right),
\end{aligned} \tag{5.28}$$

$$\left(\left(\phi^{n+\frac{1}{2}}\mathbf{D}\left(\mathbf{u}^{n+\frac{1}{2}}\right)\right)^{-1}\frac{\mathbf{s}^{n+1}+\mathbf{s}^{n}}{2},\mathbf{w}\right)=\left(\left(\phi^{n+\frac{1}{2}}\right)^{-1}\mathbf{M}_e\left(\mathbf{u}^{n+\frac{1}{2}}\right)\frac{c_f^{n+1}+c_f^{n}}{2},\mathbf{w}\right)$$
$$+\mathcal{D}\left(\frac{c_f^{n+1}+c_f^{n}}{2},\mathbf{w}\right)+\left(\varsigma_4^{n+\frac{1}{2}},\mathbf{w}\right), \tag{5.29}$$

$$\frac{\phi^{n+1}-\phi^{n}}{\tau}=\frac{1}{2}Ba_v\left(\phi^{n+1}\right)\bar{c}_f^{n+1,*}+\frac{1}{2}Ba_v\left(\phi^{n}\right)\bar{c}_f^{n}+\varsigma_5^{n}, \tag{5.30}$$

where $\zeta, v\in W_h^k$ and $\boldsymbol{\theta},\mathbf{w}\in\mathbf{W}_h^k$. Here $\varsigma_i^{n+\frac{1}{2}},(i=1,2,3,4)$ and ς_5^n are local truncation errors which satisfy

$$\left\|\varsigma_i^{n+\frac{1}{2}}\right\|\le C\tau^2,\quad \left\|\varsigma_5^{n}\right\|\le C\tau^2,\quad n\ge 1. \tag{5.31}$$

Then we can get the error equations for $n\ge 1$

$$\left(\gamma\frac{e_p^{n+1}-e_p^{n}}{\tau},\zeta\right)+\left(\frac{e_\phi^{n+1}-e_\phi^{n}}{\tau},\zeta\right)=\mathcal{L}^d\left(\frac{\mathbf{e}_{\mathbf{u}}^{n+1}+\mathbf{e}_{\mathbf{u}}^{n}}{2},\zeta\right)+\left(\varsigma_1^{n+\frac{1}{2}},\zeta\right), \tag{5.32}$$

$$\left(\frac{\rho}{\phi^{n+\frac{1}{2}}}\frac{\mathbf{u}^{n+1}-\mathbf{u}^{n}}{\tau}-\frac{\rho}{\phi_h^{n+\frac{1}{2}}}\frac{\mathbf{u}_h^{n+1}-\mathbf{u}_h^{n}}{\tau},\boldsymbol{\theta}\right)+\left(\frac{\mu}{\kappa\left(\phi^{n+\frac{1}{2}}\right)}\frac{\mathbf{u}^{n+1}+\mathbf{u}^{n}}{2}-\frac{\mu}{\kappa\left(\phi_h^{n+\frac{1}{2}}\right)}\frac{\mathbf{u}_h^{n+1}+\mathbf{u}_h^{n}}{2},\boldsymbol{\theta}\right)$$
$$+\left(\frac{\rho F(\phi^{n+\frac{1}{2}})}{\sqrt{\kappa(\phi^{n+\frac{1}{2}})}}\left|\frac{3\mathbf{u}^{n}-\mathbf{u}^{n-1}}{2}\right|\frac{\mathbf{u}^{n+1}+\mathbf{u}^{n}}{2}-\frac{\rho F(\phi_h^{n+\frac{1}{2}})}{\sqrt{\kappa(\phi_h^{n+\frac{1}{2}})}}\left|\frac{3\mathbf{u}_h^{n}-\mathbf{u}_h^{n-1}}{2}\right|\frac{\mathbf{u}_h^{n+1}+\mathbf{u}_h^{n}}{2},\boldsymbol{\theta}\right)$$
$$=\mathcal{D}\left(\frac{e_p^{n+1}+e_p^{n}}{2},\boldsymbol{\theta}\right)+\left(\varsigma_2^{n+\frac{1}{2}},\boldsymbol{\theta}\right), \tag{5.33}$$

$$\left(\frac{\phi^{n+1}c_f^{n+1}-\phi^{n}c_f^{n}-(\phi_h^{n+1}c_h^{n+1}-\phi_h^{n}c_h^{n})}{\tau},v\right)$$
$$=\mathcal{L}^d\left(\frac{\mathbf{e}_{\mathbf{s}}^{n+1}+\mathbf{e}_{\mathbf{s}}^{n}}{2},v\right)-\left(A\left(a_v\left(\phi^{n+\frac{1}{2}}\right)\frac{c_f^{n+1}+c_f^{n}}{2}-a_v\left(\phi_h^{n+\frac{1}{2}}\right)\frac{c_h^{n+1}+c_h^{n}}{2}\right),v\right)$$
$$+\left(f_p^{n+\frac{1}{2}}\frac{e_c^{n+1}+e_c^{n}}{2},v\right)+\left(\varsigma_3^{n+\frac{1}{2}},v\right), \tag{5.34}$$

$$\left(\left(\phi^{n+\frac{1}{2}}\mathbf{D}\left(\mathbf{u}^{n+\frac{1}{2}}\right)\right)^{-1}\frac{\mathbf{s}^{n+1}+\mathbf{s}^{n}}{2}-\left(\phi_h^{n+\frac{1}{2}}\mathbf{D}\left(\mathbf{u}_h^{n+\frac{1}{2},M}\right)\right)^{-1}\frac{\mathbf{s}_h^{n+1}+\mathbf{s}_h^{n}}{2},\mathbf{w}\right)$$
$$=\left(\left(\phi^{n+\frac{1}{2}}\right)^{-1}\mathbf{M}_e\left(\mathbf{u}^{n+\frac{1}{2}}\right)\frac{c_f^{n+1}+c_f^{n}}{2}-\left(\phi_h^{n+\frac{1}{2}}\right)^{-1}\mathbf{M}_e\left(\mathbf{u}_h^{n+\frac{1}{2}}\right)\frac{c_h^{n+1}+c_h^{n}}{2},\mathbf{w}\right)$$
$$+\mathcal{D}\left(\frac{e_c^{n+1}+e_c^{n}}{2},\mathbf{w}\right)+\left(\varsigma_4^{n+\frac{1}{2}},\mathbf{w}\right), \tag{5.35}$$

$$\frac{e_\phi^{n+1}-e_\phi^{n}}{\tau}=\frac{1}{2}B\left(a_v\left(\phi^{n+1}\right)c_f^{n+1,*}-a_v\left(\phi_h^{n+1}\right)\bar{c}_h^{n+1,*}\right)+\frac{1}{2}B\left(a_v\left(\phi^{n}\right)c_f^{n}-a_v\left(\phi_h^{n}\right)\bar{c}_h^{n}\right)+\varsigma_5^{n}. \tag{5.36}$$

Step 2. Multiplying (5.36) with e_ϕ^{n+1}, and then integrating it over Ω, we obtain

$$\left(e_\phi^{n+1}-e_\phi^{n},e_\phi^{n+1}\right)=\frac{\tau}{2}\left(B\left(a_v\left(\phi^{n+1}\right)-a_v\left(\phi_h^{n+1}\right)\right)c_f^{n+1,*},e_\phi^{n+1}\right)$$
$$+\frac{\tau}{2}\left(Ba_v\left(\phi_h^{n+1}\right)\left(c_f^{n+1,*}-\bar{c}_h^{n+1,*}\right),e_\phi^{n+1}\right)+\frac{\tau}{2}\left(Ba_v\left(\phi_h^{n}\right)\left(c_f^{n}-\bar{c}_h^{n}\right),e_\phi^{n+1}\right)$$
$$+\frac{\tau}{2}\left(B\left(a_v\left(\phi^{n}\right)-a_v\left(\phi_h^{n}\right)\right)c_f^{n},e_\phi^{n+1}\right)+\tau\left(\varsigma_5^{n},e_\phi^{n+1}\right). \tag{5.37}$$

Using the fact $\left|c_f^n - \bar{c}_h^n\right| \leq \left|c_f^n - c_h^n\right|$ and Lemma 2.1, we obtain

$$
\begin{aligned}
&\frac{1}{2}\left\|e_\phi^{n+1}\right\|^2 + \frac{1}{2}\left\|e_\phi^{n+1} - e_\phi^n\right\|^2 - \frac{1}{2}\left\|e_\phi^n\right\|^2 \\
&\leq C\tau\left(\left\|e_\phi^{n+1}\right\| + \left\|e_\phi^n\right\| + \left\|\xi_c^n\right\| + \left\|\xi_c^{n-1}\right\| + h^{k+1} + \tau^2\right)\left\|e_\phi^{n+1}\right\| \\
&\leq C\tau\left(\left\|e_\phi^{n+1}\right\|^2 + \left\|e_\phi^n\right\|^2 + \left\|\xi_c^n\right\|^2 + \left\|\xi_c^{n-1}\right\|^2 + h^{2k+2} + \tau^4\right).
\end{aligned} \tag{5.38}
$$

On the other hand, we have

$$
\begin{aligned}
\left\|\frac{e_\phi^{n+1} - e_\phi^n}{\tau}\right\| \leq\ & \frac{1}{2}\left\|\frac{Rc_f^{n+1,*}}{1-\phi_0} e_\phi^{n+1}\right\| + \frac{1}{2}\left\|\frac{R}{1-\phi_0}\left(1-\phi_h^{n+1}\right)\left(c_f^{n+1,*} - \bar{c}_h^{n+1,*}\right)\right\| \\
& + \frac{1}{2}\left\|\frac{Rc_f^n}{1-\phi_0} e_\phi^n\right\| + \frac{1}{2}\left\|\frac{R}{1-\phi_0}\left(1-\phi_h^n\right)\left(c_f^n - \bar{c}_h^n\right)\right\| + C\tau^2 \\
\leq\ & C\left(\left\|e_\phi^{n+1}\right\| + \left\|e_\phi^n\right\| + \left\|\xi_c^n\right\| + \left\|\xi_c^{n-1}\right\| + h^{k+1} + \tau^2\right).
\end{aligned} \tag{5.39}
$$

Step 3. Taking $\zeta = \frac{\xi_p^{n+1} + \xi_p^n}{2}$ in (5.32) and $\boldsymbol{\theta} = \frac{\boldsymbol{\xi}_{\mathbf{u}}^{n+1} + \boldsymbol{\xi}_{\mathbf{u}}^n}{2}$ in (5.33), we obtain

$$
\begin{aligned}
&\left(\gamma\frac{\xi_p^{n+1} - \xi_p^n}{\tau}, \frac{\xi_p^{n+1} + \xi_p^n}{2}\right) + \left(\frac{\rho}{\phi_h^{n+\frac{1}{2}}}\frac{\boldsymbol{\xi}_{\mathbf{u}}^{n+1} - \boldsymbol{\xi}_{\mathbf{u}}^n}{\tau}, \frac{\boldsymbol{\xi}_{\mathbf{u}}^{n+1} + \boldsymbol{\xi}_{\mathbf{u}}^n}{2}\right) + \left(\frac{\mu}{\kappa\left(\phi_h^{n+\frac{1}{2}}\right)}\frac{\boldsymbol{\xi}_{\mathbf{u}}^{n+1} + \boldsymbol{\xi}_{\mathbf{u}}^n}{2}, \frac{\boldsymbol{\xi}_{\mathbf{u}}^{n+1} + \boldsymbol{\xi}_{\mathbf{u}}^n}{2}\right) \\
&+ \left(\frac{\rho F\left(\phi_h^{n+\frac{1}{2}}\right)}{\sqrt{\kappa\left(\phi_h^{n+\frac{1}{2}}\right)}}\left|\frac{3\mathbf{u}_h^n - \mathbf{u}_h^{n-1}}{2}\right|\frac{\boldsymbol{\xi}_{\mathbf{u}}^{n+1} + \boldsymbol{\xi}_{\mathbf{u}}^n}{2}, \frac{\boldsymbol{\xi}_{\mathbf{u}}^{n+1} + \boldsymbol{\xi}_{\mathbf{u}}^n}{2}\right) = \sum_{i=1}^{7} T_i,
\end{aligned} \tag{5.40}
$$

where

$$
\begin{aligned}
T_1 &= \left(\gamma\frac{\eta_p^{n+1} - \eta_p^n}{\tau}, \frac{\xi_p^{n+1} + \xi_p^n}{2}\right) - \left(\frac{e_\phi^{n+1} - e_\phi^n}{\tau}, \frac{\xi_p^{n+1} + \xi_p^n}{2}\right), \\
T_2 &= \left(\frac{\mu}{\kappa\left(\phi_h^{n+\frac{1}{2}}\right)}\frac{\boldsymbol{\eta}_{\mathbf{u}}^{n+1} + \boldsymbol{\eta}_{\mathbf{u}}^n}{2}, \frac{\boldsymbol{\xi}_{\mathbf{u}}^{n+1} + \boldsymbol{\xi}_{\mathbf{u}}^n}{2}\right) + \left(\left(\frac{\mu}{\kappa\left(\phi_h^{n+\frac{1}{2}}\right)} - \frac{\mu}{\kappa\left(\phi^{n+\frac{1}{2}}\right)}\right)\frac{\mathbf{u}^{n+1} + \mathbf{u}^n}{2}, \frac{\boldsymbol{\xi}_{\mathbf{u}}^{n+1} + \boldsymbol{\xi}_{\mathbf{u}}^n}{2}\right), \\
T_3 &= \left(\left(\frac{\rho}{\phi_h^{n+\frac{1}{2}}} - \frac{\rho}{\phi^{n+\frac{1}{2}}}\right)\frac{\mathbf{u}^{n+1} - \mathbf{u}^n}{\tau}, \frac{\boldsymbol{\xi}_{\mathbf{u}}^{n+1} + \boldsymbol{\xi}_{\mathbf{u}}^n}{2}\right) + \left(\frac{\rho}{\phi_h^{n+\frac{1}{2}}}\frac{\boldsymbol{\eta}_{\mathbf{u}}^{n+1} - \boldsymbol{\eta}_{\mathbf{u}}^n}{\tau}, \frac{\boldsymbol{\xi}_{\mathbf{u}}^{n+1} + \boldsymbol{\xi}_{\mathbf{u}}^n}{2}\right), \\
T_4 &= -\mathcal{D}\left(\frac{\eta_p^{n+1} + \eta_p^n}{2}, \frac{\boldsymbol{\xi}_{\mathbf{u}}^{n+1} + \boldsymbol{\xi}_{\mathbf{u}}^n}{2}\right), \\
T_5 &= \left(\frac{\rho F\left(\phi_h^{n+\frac{1}{2}}\right)}{\sqrt{\kappa\left(\phi_h^{n+\frac{1}{2}}\right)}}\left(\left|\frac{3\mathbf{u}_h^n - \mathbf{u}_h^{n-1}}{2}\right| - \left|\frac{3\mathbf{u}^n - \mathbf{u}^{n-1}}{2}\right|\right)\frac{\mathbf{u}^{n+1} + \mathbf{u}^n}{2}, \frac{\boldsymbol{\xi}_{\mathbf{u}}^{n+1} + \boldsymbol{\xi}_{\mathbf{u}}^n}{2}\right) \\
&\quad + \left(\frac{\rho F\left(\phi_h^{n+\frac{1}{2}}\right)}{\sqrt{\kappa\left(\phi_h^{n+\frac{1}{2}}\right)}}\left|\frac{3\mathbf{u}_h^n - \mathbf{u}_h^{n-1}}{2}\right|\frac{\boldsymbol{\eta}_{\mathbf{u}}^{n+1} + \boldsymbol{\eta}_{\mathbf{u}}^n}{2}, \frac{\boldsymbol{\xi}_{\mathbf{u}}^{n+1} + \boldsymbol{\xi}_{\mathbf{u}}^n}{2}\right),
\end{aligned}
$$

$$T_6 = \left(\left(\frac{\rho F\left(\phi_h^{n+\frac{1}{2}}\right)}{\sqrt{\kappa\left(\phi_h^{n+\frac{1}{2}}\right)}} - \frac{\rho F\left(\phi^{n+\frac{1}{2}}\right)}{\sqrt{\kappa\left(\phi^{n+\frac{1}{2}}\right)}} \right) \left| \frac{3\mathbf{u}^n - \mathbf{u}^{n-1}}{2} \right| \frac{\mathbf{u}^{n+1} + \mathbf{u}^n}{2}, \frac{\boldsymbol{\xi}_{\mathbf{u}}^{n+1} + \boldsymbol{\xi}_{\mathbf{u}}^n}{2} \right),$$

$$T_7 = \left(\varsigma_1^{n+\frac{1}{2}}, \frac{\xi_p^{n+1} + \xi_p^n}{2} \right) + \left(\varsigma_2^{n+\frac{1}{2}}, \frac{\boldsymbol{\xi}_{\mathbf{u}}^{n+1} + \boldsymbol{\xi}_{\mathbf{u}}^n}{2} \right).$$

Now we estimate $T_i, i = 1, \cdots, 7$ term by term. Using Lemma 5.1 and (5.39), we obtain

$$T_1 \leq C\left(\|e_\phi^{n+1}\| + \|e_\phi^n\| + \|\xi_c^n\| + \|\xi_c^{n-1}\| + h^{k+1} + \tau^2\right)\left(\|\xi_p^{n+1}\| + \|\xi_p^n\|\right).$$

The estimate of T_2 requires hypothesis 3 and Lemma 2.1,

$$T_2 \leq C\left(h^{k+1} + \|e_\phi^{n+1}\| + \|e_\phi^n\|\right) \left\| \frac{\boldsymbol{\xi}_{\mathbf{u}}^{n+1} + \boldsymbol{\xi}_{\mathbf{u}}^n}{2} \right\|.$$

Using Lemma 5.1 and hypothesis 3 again, we get

$$T_3 \leq C\left(\|e_\phi^{n+1}\| + \|e_\phi^n\| + h^{k+1}\right) \left\| \frac{\boldsymbol{\xi}_{\mathbf{u}}^{n+1} + \boldsymbol{\xi}_{\mathbf{u}}^n}{2} \right\|,$$

where we have applied the boundedness of $\phi_h^{n+\frac{1}{2}}$. The estimate of T_4 follows from Lemma 3.3,

$$T_4 \leq Ch^{k+1}\|p^{n+1}\|_{k+2} \left\| \frac{\boldsymbol{\xi}_{\mathbf{u}}^{n+1} + \boldsymbol{\xi}_{\mathbf{u}}^n}{2} \right\| + Ch^{k+1}\|p^n\|_{k+2} \left\| \frac{\boldsymbol{\xi}_{\mathbf{u}}^{n+1} + \boldsymbol{\xi}_{\mathbf{u}}^n}{2} \right\|.$$

Now we estimate T_5. For the second part in T_5, we have

$$\begin{aligned}
&\left(\frac{\rho F\left(\phi_h^{n+\frac{1}{2}}\right)}{\sqrt{\kappa\left(\phi_h^{n+\frac{1}{2}}\right)}} \left| \frac{3\mathbf{u}_h^n - \mathbf{u}_h^{n-1}}{2} \right| \frac{\boldsymbol{\eta}_{\mathbf{u}}^{n+1} + \boldsymbol{\eta}_{\mathbf{u}}^n}{2}, \frac{\boldsymbol{\xi}_{\mathbf{u}}^{n+1} + \boldsymbol{\xi}_{\mathbf{u}}^n}{2} \right) \\
\leq &\left(\frac{\rho F\left(\phi_h^{n+\frac{1}{2}}\right)}{\sqrt{\kappa\left(\phi_h^{n+\frac{1}{2}}\right)}} \left| \frac{3\boldsymbol{\xi}_{\mathbf{u}}^n - \boldsymbol{\xi}_{\mathbf{u}}^{n-1}}{2} \right| \frac{\boldsymbol{\eta}_{\mathbf{u}}^{n+1} + \boldsymbol{\eta}_{\mathbf{u}}^n}{2}, \frac{\boldsymbol{\xi}_{\mathbf{u}}^{n+1} + \boldsymbol{\xi}_{\mathbf{u}}^n}{2} \right) \\
&+ \left(\frac{\rho F\left(\phi_h^{n+\frac{1}{2}}\right)}{\sqrt{\kappa\left(\phi_h^{n+\frac{1}{2}}\right)}} \left| \frac{3\boldsymbol{\eta}_{\mathbf{u}}^n - \boldsymbol{\eta}_{\mathbf{u}}^{n-1}}{2} \right| \frac{\boldsymbol{\eta}_{\mathbf{u}}^{n+1} + \boldsymbol{\eta}_{\mathbf{u}}^n}{2}, \frac{\boldsymbol{\xi}_{\mathbf{u}}^{n+1} + \boldsymbol{\xi}_{\mathbf{u}}^n}{2} \right) \\
&+ \left(\frac{\rho F\left(\phi_h^{n+\frac{1}{2}}\right)}{\sqrt{\kappa\left(\phi_h^{n+\frac{1}{2}}\right)}} \left| \frac{3\mathbf{u}^n - \mathbf{u}^{n-1}}{2} \right| \frac{\boldsymbol{\eta}_{\mathbf{u}}^{n+1} + \boldsymbol{\eta}_{\mathbf{u}}^n}{2}, \frac{\boldsymbol{\xi}_{\mathbf{u}}^{n+1} + \boldsymbol{\xi}_{\mathbf{u}}^n}{2} \right).
\end{aligned}$$

Thanks to (5.3) in Lemma 5.1, Lemma 4.3 and triangle inequality, we have

$$T_5 \leq C\left(\|\boldsymbol{\xi}_{\mathbf{u}}^n\| + \|\boldsymbol{\xi}_{\mathbf{u}}^{n-1}\| + h^{k+1}\right) \left\| \frac{\boldsymbol{\xi}_{\mathbf{u}}^{n+1} + \boldsymbol{\xi}_{\mathbf{u}}^n}{2} \right\|.$$

We estimate T_6 by Lemma 4.3,

$$T_6 \leq C\left(\|e_\phi^{n+1}\| + \|e_\phi^n\|\right) \left\| \frac{\boldsymbol{\xi}_{\mathbf{u}}^{n+1} + \boldsymbol{\xi}_{\mathbf{u}}^n}{2} \right\|.$$

Obviously,

$$T_7 \le C\tau^2\left(\left\|\xi_p^{n+1}\right\| + \left\|\xi_p^n\right\|\right) + C\tau^2\left\|\frac{\boldsymbol{\xi}_{\mathbf{u}}^{n+1}+\boldsymbol{\xi}_{\mathbf{u}}^n}{2}\right\|.$$

Substituting the above equations into (5.40), we obtain

$$\begin{aligned}
&\frac{\gamma}{2}\left\|\xi_p^{n+1}\right\|^2 - \frac{\gamma}{2}\left\|\xi_p^n\right\|^2 + \frac{1}{2}\left\|\sqrt{\frac{\rho}{\phi_h^{n+\frac{1}{2}}}}\boldsymbol{\xi}_{\mathbf{u}}^{n+1}\right\|^2 - \frac{1}{2}\left\|\sqrt{\frac{\rho}{\phi_h^{n-\frac{1}{2}}}}\boldsymbol{\xi}_{\mathbf{u}}^{n}\right\|^2 + \tau\left\|\sqrt{\frac{\mu}{\kappa(\phi_h^{n+\frac{1}{2}})}}\frac{\boldsymbol{\xi}_{\mathbf{u}}^{n+1}+\boldsymbol{\xi}_{\mathbf{u}}^n}{2}\right\|^2\\
&+\tau\left\|\left(\frac{\rho F\left(\phi_h^{n+\frac{1}{2}}\right)}{\sqrt{\kappa\left(\phi_h^{n+\frac{1}{2}}\right)}}\left|\frac{3\mathbf{u}_h^n-\mathbf{u}_h^{n-1}}{2}\right|\right)^{1/2}\frac{\boldsymbol{\xi}_{\mathbf{u}}^{n+1}+\boldsymbol{\xi}_{\mathbf{u}}^n}{2}\right\|^2\\
&\le C\tau\left(\left\|e_\phi^{n+1}\right\| + \left\|e_\phi^n\right\| + \left\|\xi_c^n\right\| + \left\|\xi_c^{n-1}\right\| + h^{k+1}+\tau^2\right)\left(\left\|\xi_p^{n+1}\right\| + \left\|\xi_p^n\right\|\right)\\
&\quad + C\tau\left(\left\|e_\phi^{n+1}\right\| + \left\|e_\phi^n\right\| + \left\|\boldsymbol{\xi}_{\mathbf{u}}^n\right\| + \left\|\boldsymbol{\xi}_{\mathbf{u}}^{n-1}\right\| + h^{k+1}+\tau^2\right)\left\|\frac{\boldsymbol{\xi}_{\mathbf{u}}^{n+1}+\boldsymbol{\xi}_{\mathbf{u}}^n}{2}\right\|\\
&\le C\tau\left(\left\|e_\phi^{n+1}\right\|^2 + \left\|e_\phi^n\right\|^2 + \left\|\xi_c^n\right\|^2 + \left\|\xi_c^{n-1}\right\|^2 + \left\|\xi_p^{n+1}\right\|^2 + \left\|\xi_p^n\right\|^2\right)\\
&\quad + C\tau\left(\left\|\boldsymbol{\xi}_{\mathbf{u}}^n\right\|^2 + \left\|\boldsymbol{\xi}_{\mathbf{u}}^{n-1}\right\|^2\right) + C\tau\left(h^{2k+2}+\tau^4\right) + \varepsilon\tau\left\|\sqrt{\frac{\mu}{\kappa(\phi_h^{n+\frac{1}{2}})}}\frac{\boldsymbol{\xi}_{\mathbf{u}}^{n+1}+\boldsymbol{\xi}_{\mathbf{u}}^n}{2}\right\|^2.
\end{aligned} \tag{5.41}$$

Here we also need the monotonicity of ϕ_h in the treatment of the fourth term on the left-hand side.

Step 4. Taking $v = \frac{\xi_c^{n+1}+\xi_c^n}{2}$ and $\mathbf{w} = \frac{\boldsymbol{\xi}_{\mathbf{s}}^{n+1}+\boldsymbol{\xi}_{\mathbf{s}}^n}{2}$ in (5.34) and (5.35) respectively and summing these two equations, we have

$$\left(\frac{\left(\xi_c^{n+1}-\xi_c^n\right)\phi_h^{n+1}}{\tau}, \frac{\xi_c^{n+1}+\xi_c^n}{2}\right) + \left(\left(\phi_h^{n+\frac{1}{2}}\mathbf{D}\left(\mathbf{u}_h^{n+\frac{1}{2},M}\right)\right)^{-1}\frac{\boldsymbol{\xi}_{\mathbf{s}}^{n+1}+\boldsymbol{\xi}_{\mathbf{s}}^n}{2}, \frac{\boldsymbol{\xi}_{\mathbf{s}}^{n+1}+\boldsymbol{\xi}_{\mathbf{s}}^n}{2}\right) = \sum_{i=1}^{6} R_i, \tag{5.42}$$

where

$$\begin{aligned}
R_1 &= \left(\frac{\left(\eta_c^{n+1}-\eta_c^n\right)\phi_h^{n+1}}{\tau}, \frac{\xi_c^{n+1}+\xi_c^n}{2}\right) - \left(\frac{\left(c_f^{n+1}-c_f^n\right)e_\phi^{n+1}}{\tau}, \frac{\xi_c^{n+1}+\xi_c^n}{2}\right)\\
&\quad - \left(\frac{\left(e_\phi^{n+1}-e_\phi^n\right)c_f^n}{\tau}, \frac{\xi_c^{n+1}+\xi_c^n}{2}\right) - \left(\frac{\left(\phi_h^{n+1}-\phi_h^n\right)\xi_c^n}{\tau}, \frac{\xi_c^{n+1}+\xi_c^n}{2}\right)\\
&\quad + \left(\frac{\left(\phi_h^{n+1}-\phi_h^n\right)\eta_c^n}{\tau}, \frac{\xi_c^{n+1}+\xi_c^n}{2}\right),\\
R_2 &= \left(\left(\left(\phi_h^{n+\frac{1}{2}}\mathbf{D}\left(\mathbf{u}_h^{n+\frac{1}{2},M}\right)\right)^{-1} - \left(\phi^{n+\frac{1}{2}}\mathbf{D}\left(\mathbf{u}^{n+\frac{1}{2}}\right)\right)^{-1}\right)\frac{\mathbf{s}^{n+1}+\mathbf{s}^n}{2}, \frac{\boldsymbol{\xi}_{\mathbf{s}}^{n+1}+\boldsymbol{\xi}_{\mathbf{s}}^n}{2}\right)\\
&\quad + \left(\left(\left(\phi^{n+\frac{1}{2}}\right)^{-1}\mathbf{M}_e\left(\mathbf{u}^{n+\frac{1}{2}}\right) - \left(\phi_h^{n+\frac{1}{2}}\right)^{-1}\mathbf{M}_e\left(\mathbf{u}_h^{n+\frac{1}{2}}\right)\right)\frac{c_f^{n+1}+c_f^n}{2}, \frac{\boldsymbol{\xi}_{\mathbf{s}}^{n+1}+\boldsymbol{\xi}_{\mathbf{s}}^n}{2}\right),\\
R_3 &= -\mathcal{D}\left(\frac{\eta_c^{n+1}+\eta_c^n}{2}, \frac{\boldsymbol{\xi}_{\mathbf{s}}^{n+1}+\boldsymbol{\xi}_{\mathbf{s}}^n}{2}\right),\\
R_4 &= \left(\left(\phi_h^{n+\frac{1}{2}}\mathbf{D}\left(\mathbf{u}_h^{n+\frac{1}{2},M}\right)\right)^{-1}\frac{\boldsymbol{\eta}_{\mathbf{s}}^{n+1}+\boldsymbol{\eta}_{\mathbf{s}}^n}{2}, \frac{\boldsymbol{\xi}_{\mathbf{s}}^{n+1}+\boldsymbol{\xi}_{\mathbf{s}}^n}{2}\right) + \left(\left(\phi_h^{n+\frac{1}{2}}\right)^{-1}\mathbf{M}_e\left(\mathbf{u}_h^{n+\frac{1}{2}}\right)\frac{e_c^{n+1}+e_c^n}{2}, \frac{\boldsymbol{\xi}_{\mathbf{s}}^{n+1}+\boldsymbol{\xi}_{\mathbf{s}}^n}{2}\right),\\
R_5 &= \left(f_p^{n+\frac{1}{2}}\frac{e_c^{n+1}+e_c^n}{2}, \frac{\xi_c^{n+1}+\xi_c^n}{2}\right) + \left(\varsigma_3^{n+\frac{1}{2}}, \frac{\xi_c^{n+1}+\xi_c^n}{2}\right) + \left(\varsigma_4^{n+\frac{1}{2}}, \frac{\boldsymbol{\xi}_{\mathbf{s}}^{n+1}+\boldsymbol{\xi}_{\mathbf{s}}^n}{2}\right),\\
R_6 &= A\left(a_v\left(\phi_h^{n+\frac{1}{2}}\right)\frac{c_h^{n+1}+c_h^n}{2} - a_v\left(\phi^{n+\frac{1}{2}}\right)\frac{c_f^{n+1}+c_f^n}{2}, \frac{\xi_c^{n+1}+\xi_c^n}{2}\right).
\end{aligned}$$

Now we estimate $R_i (i = 1, \cdots, 6)$ term by term. The estimate is similar to that in Section 5.2 in [26]. So we skip the same details and only state the estimates.

$$
\begin{aligned}
R_1 &\leq C\left(h^{k+1} + \|e_\phi^{n+1}\| + \|e_\phi^n\| + \|\xi_c^n\| + \|\xi_c^{n-1}\| + \tau^2\right)\left(\|\xi_c^{n+1}\| + \|\xi_c^n\|\right),\\
R_2 &\leq C\left(\|\boldsymbol{\xi}_{\mathbf{u}}^{n+1}\| + \|\boldsymbol{\xi}_{\mathbf{u}}^n\| + \|e_\phi^{n+1}\| + \|e_\phi^n\| + h^{k+1}\right)\left\|\frac{\boldsymbol{\xi}_{\mathbf{s}}^{n+1} + \boldsymbol{\xi}_{\mathbf{s}}^n}{2}\right\|,\\
R_3 &\leq Ch^{k+1}\left\|c_f^{n+1}\right\|_{k+2}\left\|\frac{\boldsymbol{\xi}_{\mathbf{s}}^{n+1} + \boldsymbol{\xi}_{\mathbf{s}}^n}{2}\right\| + Ch^{k+1}\left\|c_f^n\right\|_{k+2}\left\|\frac{\boldsymbol{\xi}_{\mathbf{s}}^{n+1} + \boldsymbol{\xi}_{\mathbf{s}}^n}{2}\right\|,\\
R_4 &\leq C\left(\|\xi_c^{n+1}\| + \|\xi_c^n\| + h^{k+1}\right)\left\|\frac{\boldsymbol{\xi}_{\mathbf{s}}^{n+1} + \boldsymbol{\xi}_{\mathbf{s}}^n}{2}\right\|,\\
R_5 &\leq C\left(\|\xi_c^{n+1}\| + \|\xi_c^n\| + h^{k+1} + \tau^2\right)\left(\|\xi_c^{n+1}\| + \|\xi_c^n\|\right) + C\tau^2\left\|\frac{\boldsymbol{\xi}_{\mathbf{s}}^{n+1} + \boldsymbol{\xi}_{\mathbf{s}}^n}{2}\right\|,\\
R_6 &\leq C\left(\|\xi_c^{n+1}\| + \|\xi_c^n\| + \|e_\phi^{n+1}\| + \|e_\phi^n\| + h^{k+1}\right)\left(\|\xi_c^{n+1}\| + \|\xi_c^n\|\right).
\end{aligned}
$$

Substituting the above equations into (5.42) and using Young's inequality, we have

$$
\begin{aligned}
&\frac{1}{2}\left\|\sqrt{\phi_h^{n+1}}\xi_c^{n+1}\right\|^2 - \frac{1}{2}\left\|\sqrt{\phi_h^n}\xi_c^n\right\|^2 + \tau\left\|\left(\phi_h^{n+\frac{1}{2}}\mathbf{D}\left(\mathbf{u}_h^{n+\frac{1}{2},M}\right)\right)^{-1/2}\frac{\boldsymbol{\xi}_{\mathbf{s}}^{n+1} + \boldsymbol{\xi}_{\mathbf{s}}^n}{2}\right\|^2\\
&\leq C\tau\left(\|e_\phi^{n+1}\|^2 + \|e_\phi^n\|^2 + \|\xi_c^{n+1}\|^2 + \|\xi_c^n\|^2 + \|\xi_c^{n-1}\|^2 + \|\boldsymbol{\xi}_{\mathbf{u}}^{n+1}\|^2 + \|\boldsymbol{\xi}_{\mathbf{u}}^n\|^2\right)\\
&\quad + \varepsilon\tau\left\|\left(\phi_h^{n+\frac{1}{2}}\mathbf{D}(\mathbf{u}_h^{n+\frac{1}{2},M})\right)^{-1/2}\frac{\boldsymbol{\xi}_{\mathbf{s}}^{n+1} + \boldsymbol{\xi}_{\mathbf{s}}^n}{2}\right\|^2 + C\tau\left(h^{2k+2} + \tau^4\right),
\end{aligned}
\tag{5.43}
$$

where the treatment of the second term on the left-hand side is similar to (4.54). Taking $\varepsilon = \frac{1}{8}$, combining (5.38), (5.41) and (5.43) and summing it over n, we obtain

$$
\begin{aligned}
&\frac{1}{2}\|e_\phi^{n+1}\|^2 + \frac{\gamma}{2}\|\xi_p^{n+1}\|^2 + \frac{1}{2}\left\|\sqrt{\phi_h^{n+1}}\xi_c^{n+1}\right\|^2 + \frac{1}{2}\left\|\sqrt{\frac{\rho}{\phi_h^{n+\frac{1}{2}}}}\boldsymbol{\xi}_{\mathbf{u}}^{n+1}\right\|^2 + \frac{7\tau}{8}\sum_{m=1}^{n}\left\|\sqrt{\frac{\mu}{\kappa(\phi_h^{m+\frac{1}{2}})}}\frac{\boldsymbol{\xi}_{\mathbf{u}}^{m+1} + \boldsymbol{\xi}_{\mathbf{u}}^m}{2}\right\|^2\\
&\quad + \tau\sum_{m=1}^{n}\left\|\left(\frac{\rho F\left(\phi_h^{m+\frac{1}{2}}\right)}{\sqrt{\kappa\left(\phi_h^{m+\frac{1}{2}}\right)}}\left|\frac{3\mathbf{u}_h^m - \mathbf{u}_h^{m-1}}{2}\right|\right)^{1/2}\frac{\boldsymbol{\xi}_{\mathbf{u}}^{m+1} + \boldsymbol{\xi}_{\mathbf{u}}^m}{2}\right\|^2\\
&\quad + \frac{7\tau}{8}\sum_{m=1}^{n}\left\|\left(\phi_h^{m+\frac{1}{2}}\mathbf{D}\left(\mathbf{u}_h^{m+\frac{1}{2},M}\right)\right)^{-1/2}\frac{\boldsymbol{\xi}_{\mathbf{s}}^{m+1} + \boldsymbol{\xi}_{\mathbf{s}}^m}{2}\right\|^2\\
&\leq C\tau\sum_{m=1}^{n}\left(\|e_\phi^{m+1}\|^2 + \|e_\phi^m\|^2 + \|\xi_c^{m+1}\|^2 + \|\xi_c^m\|^2 + \|\xi_c^{m-1}\|^2 + \|\xi_p^{m+1}\|^2 + \|\xi_p^m\|^2\right)\\
&\quad + C\tau\sum_{m=1}^{n}\left(\|\boldsymbol{\xi}_{\mathbf{u}}^{m+1}\|^2 + \|\boldsymbol{\xi}_{\mathbf{u}}^m\|^2 + \|\boldsymbol{\xi}_{\mathbf{u}}^{m-1}\|^2\right) + C\left(h^{2k+2} + \tau^4\right) + Q_1,
\end{aligned}
\tag{5.44}
$$

where

$$
Q_1 = \frac{1}{2}\|e_\phi^1\|^2 + \frac{\gamma}{2}\|\xi_p^1\|^2 + \frac{1}{2}\left\|\sqrt{\phi_h^1}\xi_c^1\right\|^2 + \frac{1}{2}\left\|\sqrt{\frac{\rho}{\phi_h^{\frac{1}{2}}}}\boldsymbol{\xi}_{\mathbf{u}}^1\right\|^2 \leq C\left(h^{2k+2} + \tau^4\right).
\tag{5.45}
$$

We can prove (5.45) with Lemma 5.5. Under the condition $C\tau \leq min(\frac{1}{4}, \frac{\gamma}{4}, \frac{\rho}{4}, \frac{\phi_*}{4})$, we can get (5.24) by applying discrete Gronwall's inequality to (5.44).

Finally, by using the standard approximation result, we obtain (5.25). □

Table 1
Accuracy test for the Fully-LDG(k,r)(r = 1,2) scheme of the wormhole propagations.

Time scheme	N	$\|p-p_h\|$	Order	$\|u-u_h\|$	Order	$\|c_f-c_{fh}\|$	Order	$\|\phi-\phi_h\|$	Order
First order	16	8.21E−3	–	5.60E−3	–	3.70E−3	–	3.56E−5	–
	32	2.38E−3	1.79.	1.46E−3	1.93	1.13E−3	1.71	1.01E−5	1.81
	64	7.77E−4	1.61.	4.01E−4	1.86	4.33E−4	1.38	3.45E−6	1.55
	128	3.15E−4	1.30.	1.29E−4	1.63	1.97E−4	1.14	1.46E−6	1.24
Second order	16	7.69E−3	–	5.78E−3	–	3.33E−3	–	3.45E−5	–
	32	2.52E−3	1.61	1.58E−3	1.87	8.37E−4	2.01	8.68E−6	1.99
	64	6.54E−4	1.95	4.00E−4	1.98	2.09E−4	2.00	2.18E−6	2.00
	128	1.52E−4	2.10	9.87E−5	2.01	5.22E−5	2.00	5.45E−7	2.00

6. Numerical experiments

In this section, we perform several numerical examples to illustrate the accuracy and capability of the fully-discrete schemes (4.14)–(4.25) for wormhole propagations.

6.1. Accuracy test

Example 6.1. We solve (2.1)–(2.4) and the parameters are taken as

$$\begin{aligned}&d_m=10^{-2},\ \alpha_l=0,\ \alpha_t=0,\ K_0=1,\ T=0.2,\\&\alpha=k_c=k_s=\mu=1,\ f_p=f_l=0,\ \rho=1,\\&a_0=0.5,\ \rho_s=10,\ \gamma=1.\end{aligned} \tag{6.1}$$

The exact smooth solutions are given as

$$\begin{aligned}&p(\mathbf{x},t)=e^{-t}\cos(2\pi x)\cos(2\pi y),\quad \mathbf{u}(\mathbf{x},t)=e^{-t}[\sin(2\pi x)\cos(2\pi y);\cos(2\pi x)\sin(2\pi y)],\\&\phi(\mathbf{x},t)=0.6+t^2\sin(2\pi x)\cos(2\pi y),\quad c_f(\mathbf{x},t)=0.5+0.1e^{-t}\sin(2\pi x)\sin(2\pi y).\end{aligned} \tag{6.2}$$

We can calculate the initial conditions and the right hand sides accordingly. Piecewise linear tensor product polynomials are employed in the LDG scheme. We perform accuracy verifications on uniform meshes with $N\times N$ elements over the computational domain $\Omega=[0,1]\times[0,1]$, and compute the numerical approximations at $T=0.2$. The time step is taken as $\tau=0.1$ h, $h=\frac{1}{N}$. Periodic boundary condition is used in this numerical example. The numerical results for the error in L^2 norm and corresponding order of accuracy are presented in Table 1. From the table, we can observe optimal convergence rates, which verifies the theoretical results.

6.2. Wormhole propagation problem

This is a real wormhole propagation scenario in petroleum engineering. The computational domain is $\Omega=[0,0.2\text{ m}]\times[0,0.2\text{ m}]$. Initial concentration of acid and initial porosity of rock in this domain are set to be $c_0=0$ and $\phi_0=0.2$, respectively. The acid flow is injected to the porous media from the left boundary with a velocity of 0.01 m/s and drained out of it from the right boundary with the same velocity. The velocity is defined as $\mathbf{u}=[0.01,0]^T$ m/s. Top and bottom boundary conditions are set to be periodic. The concentration of influx acid is 1 mole/m^2. To observe the wormhole propagation, we set two square singular areas with high porosity and permeability on the left boundary with width 0.01 m: one is 0.05 m above the bottom with the porosity of 0.4, and the other 0.1 m above the bottom with the porosity of 0.6. The permeability of the two entries is determined by (2.7) which is about 10^{-10} m^2 and 10^{-11} m^2, respectively.

Example 6.2. A real wormhole propagation scenario in petroleum engineering is studied in this example. The parameters are taken as

$$\begin{aligned}&d_m=10^{-5},\quad \alpha_l=0,\quad \alpha_t=0,\quad K_0=10^{-9}\text{ m}^2,\quad T=50\text{ s},\\&\alpha=100\text{ kg/mol},\quad k_c=1\text{ m/s},\quad k_s=10\text{ m/s},\\&\mu=10^{-2}\text{ Pa s},\quad f_l=f_p=0,\quad \rho=1000,\\&a_0=2\text{ m}^{-1},\quad \rho_s=2500\text{ kg/m}^2,\quad \gamma=0.01.\end{aligned} \tag{6.3}$$

In this example, the Fully-LDG(k,2) is employed, and the time step is chosen as $\tau=0.2h$ with uniform mesh size h. The LDG discretization with linear polynomial is used in this example. The contour plots of concentration of acid, porosity of rock and pressure on a uniform mesh with 80 × 80 elements at different time are shown in Fig. 1. We can clearly see the wormhole generates and grows with time.

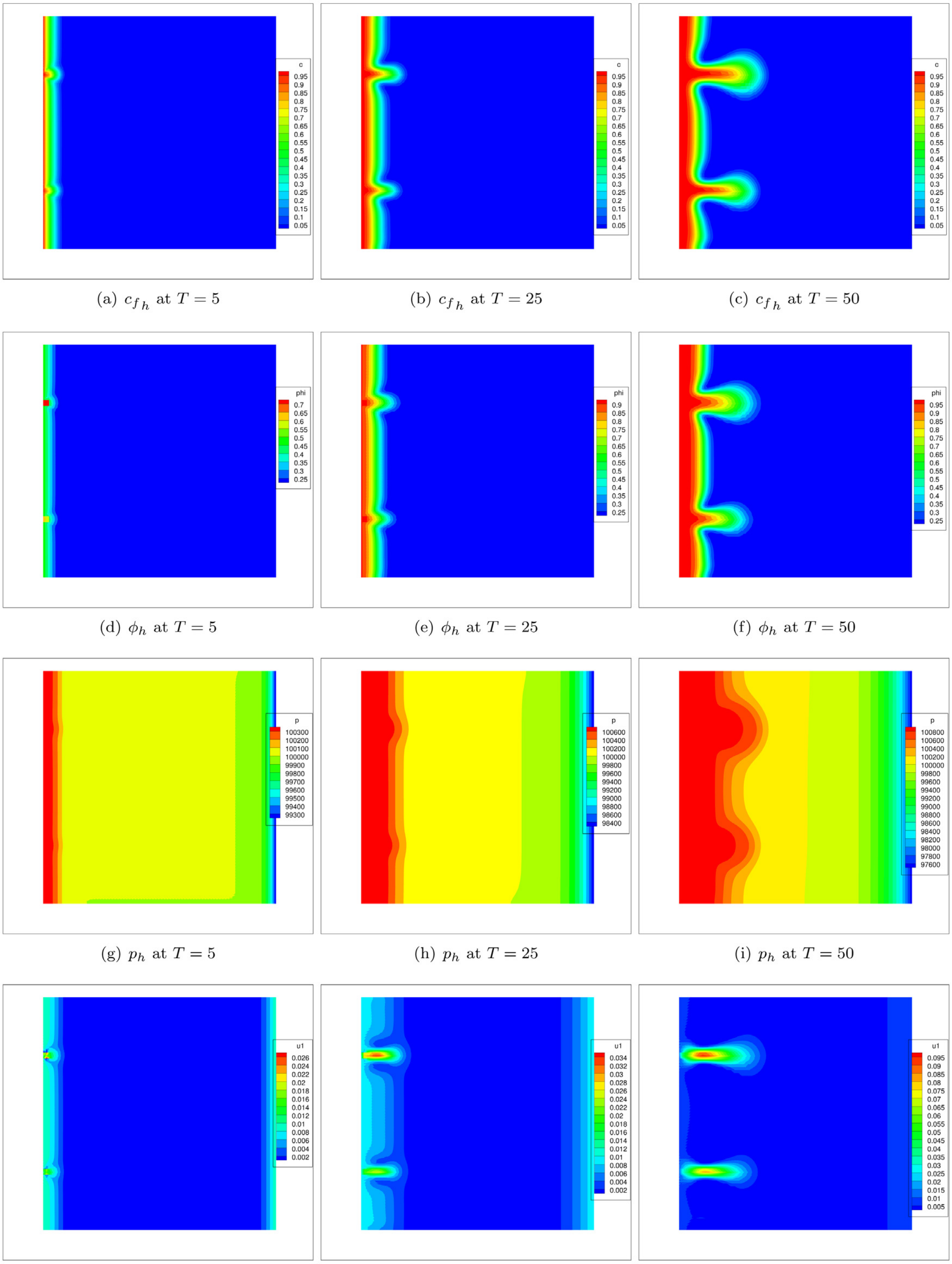

(a) ${c_f}_h$ at $T = 5$ (b) ${c_f}_h$ at $T = 25$ (c) ${c_f}_h$ at $T = 50$

(d) ϕ_h at $T = 5$ (e) ϕ_h at $T = 25$ (f) ϕ_h at $T = 50$

(g) p_h at $T = 5$ (h) p_h at $T = 25$ (i) p_h at $T = 50$

(j) u_h at $T = 5$ (k) u_h at $T = 25$ (l) u_h at $T = 50$

Fig. 1. Example 6.2: Numerical solutions for concentration, porosity, pressure and velocity along x direction at different time. The computational mesh is composed by 80×80 elements. The Fully-LDG (k,2) scheme (4.20)–(4.25) is employed with $\tau = 0.2h$.

7. Concluding remarks

In this paper, we applied the LDG spatial discretization coupled with two time integrations to wormhole propagation with Darcy–Forchheimer model. We applied a special way for the time integration of the porosity, leading to physically relevant numerical approximations and controllable growth rate of the porosity. We also proposed two suitable time integrations up to second-order accuracy. Moreover, we obtained the stability of the two schemes and proved the optimal error estimates for the pressure, velocity, porosity and concentration in different norms.

References

[1] C. Zhao, B.E. Hobbs, P. Hornb, A. Ord, S. Peng, L. Liu, Theoretical and numerical analyses of chemical-dissolution front instability in fluid-saturated porous rocks, Int. J. Numer. Anal. Methods Geom. 32 (2008) 1107–1130.
[2] P. Maheshwari, V. Balakotaiah, 3D Simulation of Carbonate Acidization with HCl: Comparison with Experiments, Society of Petroleum Engineers, 2013.
[3] Y. Wu, A. Salama, S. Sun, Parallel simulation of wormhole propagation with the Darcy-Brinkman-Forchheimer framework, Comput. Geotech. 69 (2015) 564–577.
[4] X. Li, H. Rui, Block-centered finite difference method for simulating compressible wormhole propagation, J. Sci. Comput. 74 (2018) 1115–1145.
[5] J. Zhang, X. Shen, H. Guo, H. Fu, H. Han, Characteristic splitting mixed finite element analysis of compressible wormhole propagation, Appl. Numer. Math. 147 (2020) 66–87.
[6] D. Ruth, H. Ma, On the derivation of the forchheimer equation by means of the averaging theorem, Transp. Porous Media 7 (1992) 255–264.
[7] V. Girault, M. Wheeler, Numerical discretization of a Darcy-Forchheimer model, Numer. Math. 110 (2008) 161–198.
[8] W. Liu, J. Cui, A two-grid block-centered finite difference algorithm for nonlinear compressible Darcy-Forchheimer model in porous media, J. Sci. Comput. 74 (2018) 1786–1815.
[9] H. Pan, H. Rui, Mixed element method for two-dimensional Darcy-Forchheimer model, J. Sci. Comput. 52 (2012) 563–587.
[10] H. Rui, W. Liu, A two-grid block-centered finite difference method for Darcy-Forchheimer flow in porous media, SIAM J. Numer. Anal. 53 (2015) 1941–1962.
[11] H. Rui, H. Pan, A block-centered finite difference method for slightly compressible Darcy-Forchheimer flow in porous media, J. Sci. Comput. 73 (2017) 70–92.
[12] H. Opez, M. Brígida, S. José, Comparison between different numerical discretizations for a Darcy-forchheimer model, Electron. Trans. Numer. Anal. Etna 34 (2008) 187–203.
[13] Q. Zhao, H. Rui, W. Liu, Cell-centered finite difference method for the one-dimensional Forchheimer laws, Bull. Malays. Math. Sci. Soc. 40 (2017) 545–564.
[14] J. Kou, S. Sun, Y. Wu, Mixed finite element-based fully conservative methods for simulating wormhole propagation, Comput. Methods Appl. Mech. Engrg. 298 (2016) 279–302.
[15] X. Li, H. Rui, A fully conservative finite difference method for simulating Darcy-Forchheimer compressible wormhole propagation, Numer. Algorithms 82 (2019) 451–478.
[16] W.H. Reed, T.R. Hill, Triangular Mesh Method for the Neutron Transport Equation, Technical report LA-UR-73-479, Los Alamos Scientific Laboratory, Los Alamos, NM, 1973.
[17] F. Bassi, S. Rebay, A high-order accurate discontinuous finite element method for the numerical solution of the compressible Navier–Stokes equations, J. Comput. Phys. 131 (1997) 267–279.
[18] B. Cockburn, C.-W. Shu, The local discontinuous Galerkin method for time-dependent convection–diffusion systems, SIAM J. Numer. Anal. 35 (1998) 2440–2463.
[19] H. Guo, L. Tian, Z. Xu, Y. Yang, N. Qi, High-order local discontinuous Galerkin method for simulating wormhole propagation, J. Comput. Appl. Math. 350 (2019) 247–261.
[20] L. Tian, H. Guo, R. Jia, Y. Yang, An h-adaptive local discontinuous Galerkin method for simulating wormhole propagation with Darcy-Forcheiner model, J. Sci. Comput. 82 (2020) 43.
[21] H. Wang, C.-W. Shu, Q. Zhang, Stability and error estimates of local discontinuous Galerkin methods with implicit-explicit time-marching for advection-diffusion problems, SIAM J. Numer. Anal. 53 (2015) 206–227.
[22] H. Wang, C.-W. Shu, Q. Zhang, Stability analysis and error estimates of local discontinuous Galerkin methods with implicit-explicit time-marching for nonlinear convection–diffusion problems, Appl. Math. Comput. 272 (2016) 237–258.
[23] H. Wang, S. Wang, Q. Zhang, C.-W. Shu, Local discontinuous Galerkin methods with implicit-explicit time marching for multi-dimensional convection–diffusion problems, ESAIM: M2AN 50 (2016) 1083–1105.
[24] H. Wang, Q. Zhang, S. Wang, et al., Local discontinuous Galerkin methods with explicit-implicit-null time discretizations for solving nonlinear diffusion problems, Sci. China(Mathematics) 063 (2020) 183–204.
[25] H. Wang, J. Zheng, F. Yu, H. Guo, Q. Zhang, Local discontinuous Galerkin method with implicit-explicit time marching for incompressible miscible displacement problem in porous media, J. Sci. Comput. 78 (2019) 1–28.
[26] H. Guo, R. Jia, L. Tian, Y. Yang, Stability and error estimates of local discontinuous Galerkin method with implicit-explicit time marching for simulating wormhole propagation, Math. Model. Numer. Anal. accepted.
[27] S. Mauran, L. Rigaud, O. Coudevylle, Application of the carman-kozeny correlation to a highporosity and anisotropic consolidated medium: The compressed expanded natural graphite, Transp. Porous Media 43 (2001) 355–376.
[28] P. Ciarlet, The Finite Element Method for Elliptic Problem, North Holland, 1975.
[29] P. Castillo, B. Cockburn, I. Perugia, D. Schötzau, Superconvergence of the local discontinuous Galerkin method for elliptic problems on cartesian grids, SIAM J. Numer. Anal. 39 (2001) 264–285.
[30] X. Li, C.-W. Shu, Y. Yang, Local discontinuous Galerkin method for the Keller–Segel chemotaxis model, J. Sci. Comput. 73 (2017) 943–967.